PHYSICAL REVIEW B VOLUME 21, NUMBER 4 15 FEBRUARY 1980

Tight-binding Green's functions for surfaces, thin films, and solid interfaces. A random-walk theory approach

Alberto Robledo and Carmen Varea*

División de Estudios Superiores, Facultad de Química, Universidad Nacional Autónoma de México, México 20, D. F.

(Received 27 November 1978)

We present a formalism, derived with the aid of random-walk theory, which yields the Green's function for a system with planar defects in terms of the associated bulk Green's functions. Exact analytical expressions are obtained for semi-infinite, thin-film, and solid-solid-interface systems. From these, we calculated the local density of states for (a) the (100), (110), and (111) surfaces of a model of rocksalt (two interwoven fcc sublattices with nearest-neighbor interactions); (b) a transition-metal film modeled by a two-band bcc structure; and (c) a solid interface formed by joining two semi-infinite sc one-band regions. Our results are compared with the corresponding bulk properties.

I. INTRODUCTION

The knowledge of the local density of states (LDOS) is of importance in many surface problems because it provides a way of computing electronic properties of the system without needing to know its eigenstates. Consequently, considerable effort has been put into developing reliable methods for its direct calculation. Among these, those that have in common the employment of tight-binding Hamiltonians have proved to be very productive in the study of the electronic structure of surfaces.

The various techniques for calculating the LDOS in the tight-binding approximation (and which do not require the evaluation of the state functions) can be classified into two general categories. In the first we include those methods which take advantage of the two-dimensional periodicity of the crystal along directions parallel to the surface.[1,2] By means of Bloch's theorem the three-dimensional problem is seen to take on the same form as a one-dimensional problem. The associated Green's function is obtained in terms of a wave vector parallel to the surface, and an integration on a surface Brillouin zone (SBZ), corresponding to the arrangement of atoms in the surface planes, becomes necessary. The second category includes those procedures based on path- or walk-counting techniques on a cluster of atoms near the surface. The methods of Cyrot-Lackmann[3] and of Haydock *et al.*[4] belong to this category. In both methods, the diagonal elements of the Green's function are given by a continued-fraction expression. The moment method of Cyrot-Lackmann constructs the continued fraction from the first moments of the density of states. These in turn are calculated by computing all the possible closed walks on the cluster of atoms. In the method of Haydock *et al.* the counting of walks is performed through a recursion procedure defining a unitary transformation which takes the Hamiltonian matrix into a tridiagonal matrix.[4]

The main disadvantage of the walk-counting methods is that, when accuracy in the results (e.g., near the singularities of the density of states) requires large sizes of clusters, the necessary computations may become impractical. However, their range of applicability is quite ample, for it is always possible to calculate the first few moments or iterations in complicated situations which may include the consideration of surface dilation,[4,5] adatoms or layers of adatoms,[6,7] degenerate bands,[8] stepped surfaces,[9] etc.

On the other hand, for some simple crystals with only one limiting surface (clean and unrelaxed), the methods that make use of Bloch's theorem yield closed expressions for the LDOS in terms of the bulk Green's function.[2,10] More realistic surfaces need more attention and their analysis has been complemented with some special techniques such as the transfer matrix approach.[11] However, when this approach is extended to treat crystal films one is led to iterative procedures.[12] Bloch's-theorem method has been applied recently to the study of chemisorption by calculating the change on the LDOS due to the interaction of the adatom with the clean surface.[13] Also, the effect of direct adatom-adatom interactions was obtained from a Dyson equation which couples the Green's function of a clean surface with that of a monolayer of adatoms.[14] In spite of these developments, all of the work to date[1-14] has been confined to calculations on specific crystal models [often for (100) surfaces on sc crystals with nearest-neighbor one-electron Hamiltonians] and thus the general validity of their results (particularly those which appear in closed analytical form) has not been fully explored.

Parallel to this and motivated by other problems bearing a similar mathematical structure, such as in lattice dynamics, the theory of random walks on lattices has been developed with the aid of the concept of probability generating functions.[15] Here, by showing that the electronic Green's function for a general mixed crystal can be identified with a random-walk generating function for the same lattice structure, we exhibit an explicit link between the two classes of methods referred to above. The advantage in introducing the analytical techniques of random-walk theory into the study of the tight-binding approximation becomes apparent from the simplicity of the analysis of defects in complicated lattices. We emphasize its use in discussing the effect of planar defects, surface or interface.

In Sec. II the formalism is presented in a sufficiently general framework to take into account interactions extending to any order of neighbors in a multiband crystal made up of more than one type of atom. Expressions are derived for the Green's function associated with an arbitrary set of vacancy defects in terms of that for the perfect lattice. In Secs. III and IV we particularize these expressions to the cases of semi-infinite and thin-film crystals, i.e., when the defects, or traps for the walker, constitute one or more planes of the lattice sites. In Sec. III we present the calculations for the LDOS generated by the introduction of a cleavage plane along different crystallographic directions on a crystal model featuring rocksalt (two interwoven fcc sublattices with one interacting orbital per site). In Sec. IV we study the density of states for a thin-film geometry and choose as an example a metal represented by a two-band bcc structure.

The final application of random-walk theory is to the calculation of the Green's function of a solid-solid interface. We show in Sec. V how the interface problem is solved by expressing the walks on the interface system in terms of the walks on each semi-infinite region. A slight modification of this problem, the coupling of a thin film with a one-surface crystal, yields the Green's function for a model of multilayer adsorption. We present results for a simple cubic structure. Only unrelaxed and unreconstructed surfaces (or interfaces) are examined. In Sec. VI we summarize our results and discuss how the modifications on the LDOS due to surface relaxation effects can be incorporated.

We feel that the random-walk approach to the LDOS offers considerable advantages over a direct application of Dyson's equation, for it provides a clear and systematic way of relating local to bulk Green's functions. This is particularly useful in the analysis of complicated crystals. Traditionally, the desired features of the "perturbed" system are build into the starting Green's function and the analysis is carried on by means of successive Dyson-like equations. While the general idea of this method is straightforward the formal development is rather complicated. We find it helpful to visualize a surface or interface problem in terms of its associated random-walk nature. By identifying which families of walks, taking place in the infinite perfect lattice, have to be eliminated from, or need to be included in, the description of the perturbed system we construct the appropriate Green's function. (See also Ref. 16.) A preliminary account of the random-walk approach, restricted to one-band crystals with a surface formed along a plane of symmetry, will appear elsewhere.[16]

II. GENERAL FORMALISM

A. Bulk properties

To help us study the electronic properties of a crystal consisting of several kinds of atoms, each of which possibly contains more than one interacting orbital, we consider a random-walk problem on a lattice with the following structure: Let the framework of the crystal be an infinite simple cubic lattice, the sites of which are identified by the vectors $\{\vec{s}\}$. The lattice is divided into a given number of interwoven sublattices $\{\Gamma_j\}$ labeled by the numbers $\{j\}$. The sites of a given sublattice are all occupied by the same type of atom, but different sublattices might either be occupied by different types of atoms or be empty. We consider atoms to be different when they are either of a different chemical species or when they occupy inequivalent sites on the crystal. Thus, for example, to study rocksalt or nickel one would choose two interwoven fcc lattices. For the former crystal each sublattice is occupied by one type of atom, whereas for the latter, one sublattice is empty. As an example of a crystal that forms a lattice for which the geometry yields inequivalent sites, such as diamond, we display in Fig. 1 the equivalent arrangement of sites for the hexagonal lattice on the square lattice. The numbers $\{\alpha\}$ will be used to identify the orbitals in an atom.

The first statistical question to be considered is the following: Let a random walker be at site $(\alpha', j', \vec{s}')$ initially; what is the probability that after n steps it will be at $(\alpha, j, \vec{s})$ when the various transition probabilities are known? We define $P_n(\alpha, j, \vec{s}; \alpha', j', \vec{s}')$ as the required probability and find it convenient to introduce the supermatrix $P_n(\vec{s}, \vec{s}')$ whose elements are $P_n(\alpha, j, \vec{s}; \alpha', j', \vec{s}')$.

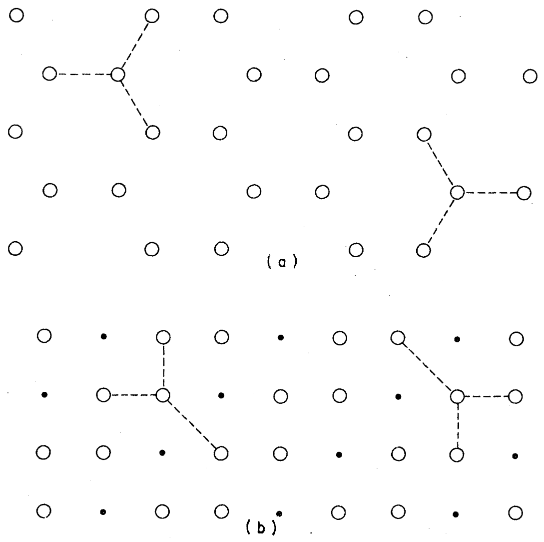

FIG. 1. Equivalent arrangement of sites for the hexagonal lattice on the square lattice: (a) Hexagonal lattice, (b) square lattice.

The transition probabilities which will apply at every step are denoted by $\{p_{jl}^{\alpha\beta}(\vec{s},\vec{s}\,')\}$, where the exhibited member of the set represents the probability that a walker at $(\beta, l, \vec{s}\,')$ will on its next step arrive at $(\alpha, j, \vec{s})$. We have the initial condition

$$P_0(\alpha,j,\vec{s};\,\alpha',j',\vec{s}\,')=\delta_{\alpha\alpha'}\delta_{jj'}\delta_{\vec{s}\vec{s}\,'} \qquad (1)$$

and the recursion formula

$$P_{n+1}(\vec{s},\vec{s}\,')=\sum_{\vec{s}\,''}p(\vec{s},\vec{s}\,'')P_n(\vec{s}\,'',\vec{s}\,')\,, \qquad (2)$$

where $p(\vec{s},\vec{s}\,')$ is the supermatrix associated with the $\{p_{jl}^{\alpha\beta}(\vec{s},\vec{s}\,')\}$.

It is useful to construct the generating function

$$P(\vec{s},\vec{s}\,';z)=\sum_{n=0}^{\infty}P_n(\vec{s},\vec{s}\,')z^n\,, \qquad (3)$$

so that from (1) and (2) we obtain the Green's-function equation

$$P(\vec{s},\vec{s}\,';z)-z\sum_{\vec{s}\,''}p(\vec{s},\vec{s}\,'')P(\vec{s}\,'',\vec{s}\,';z)=P_0(\vec{s},\vec{s}\,')\,. \qquad (4)$$

Given the translational invariance of our sc lattice framework, both $p(\vec{s},\vec{s}\,')$ and $P(\vec{s},\vec{s}\,';z)$ depend only on the displacement $\vec{s}-\vec{s}\,'$, and therefore Eq. (4) can be solved for the generating function by the application of standard Fourier-transformation formulas. Thus, if

$$\Lambda(\vec{k})=\sum_{\vec{s}}p(\vec{s})e^{i\vec{k}\cdot\vec{s}} \qquad (5)$$

and

$$U(\vec{k};z)=\sum_{\vec{s}}P(\vec{s};z)e^{i\vec{k}\cdot\vec{s}}\,, \qquad (6)$$

we have

$$P(\vec{s};z)=\frac{1}{(2\pi)^3}\int\int_0^{2\pi}\int[I-z\Lambda(\vec{k})]^{-1}e^{-i\vec{k}\cdot\vec{s}}\,d\vec{k}\,. \qquad (7)$$

In particular, when one considers two sublattices and only one orbital per site or, equivalently, no sublattice division but two orbitals per site, one has

$$\Lambda(\vec{k})\equiv\sum_{\vec{s}}\begin{bmatrix}p_{11}(\vec{s}) & p_{12}(\vec{s})\\ p_{21}(\vec{s}) & p_{22}(\vec{s})\end{bmatrix}e^{i\vec{k}\cdot\vec{s}}\equiv\begin{bmatrix}\lambda_{11}(\vec{k}) & \lambda_{12}(\vec{k})\\ \lambda_{21}(\vec{k}) & \lambda_{22}(\vec{k})\end{bmatrix} \qquad (8)$$

and

$$[I-z\Lambda(\vec{k})]^{-1}=[\det(\vec{k};z)]^{-1}\begin{bmatrix}1-z\lambda_{22}(\vec{k}) & z\lambda_{12}(\vec{k})\\ z\lambda_{21}(\vec{k}) & 1-z\lambda_{11}(\vec{k})\end{bmatrix}, \qquad (9)$$

where

$$\det(\vec{k};z)=[1-z\lambda_{11}(\vec{k})][1-z\lambda_{22}(\vec{k})]-z^2\lambda_{12}(\vec{k})\lambda_{21}(\vec{k})\,.$$

The generalization of this to the case of more than two sublattices or more orbitals per site is obvious.

We shall show next how the bulk electronic Green's function, $G(\vec{s},\vec{s}\,';E)$, for a general tight-binding Hamiltonian is related to the random-walk generating function (3). This Hamiltonian can be expressed by the supermatrix $H(\vec{s},\vec{s}\,')$ whose element $H_{jl}^{\alpha\beta}(\vec{s},\vec{s}\,')$ represents the overlap or hopping integral between states $|\phi_j^\alpha\rangle$ and $|\phi_l^\beta\rangle$ centered on lattice sites $\vec{s}$ and $\vec{s}\,'$, respectively. The elements $H_{jj}^{\alpha\beta}(\vec{s},\vec{s})$, when different from zero, represent hybridization, whereas $H_{jj}^{\alpha\alpha}(\vec{s},\vec{s})$ is the electronic energy ϵ_j^α associated with $|\phi_j^\alpha\rangle$. The Green's-function equation

$$EG(\vec{s},\vec{s}\,';E)-\sum_{\vec{s}\,''}H(\vec{s},\vec{s}\,'')G(\vec{s}\,'',\vec{s}\,';E)=\delta_{\vec{s},\vec{s}\,'}I \qquad (10)$$

is seen to be equivalent to (4) if we assume $H(\vec{s},\vec{s}\,')\equiv p(\vec{s},\vec{s}\,')$, $E\equiv z^{-1}$, and $EG(\vec{s},\vec{s}\,';E)\equiv P(\vec{s},\vec{s}\,';z)$. And thus, we obtain an algorithm relating the electronic properties of the crystal to those of a formal random-walk problem.[17] This fact has been recognized, directly or indirectly, by several authors,[3,4] and forms the basis of the moment method of Cyrot-Lackmann to calculate densities of states. The density of states per atom for the Hamiltonian

$H(\vec{s},\vec{s}\,')$ is given by

$$D_j(E) = -\frac{1}{\pi}\mathrm{Im}\sum_{\alpha} G(\alpha,j,\vec{s};\alpha,j,\vec{s};E),\quad \vec{s}\in\Gamma_j \tag{11}$$

where the energy E has a small imaginary part. The nth moment of the density of states is

$$\begin{aligned}\mu_j^{(n)} &= \int_{-\infty}^{\infty} E^n D_j(E)\,dE \\ &= \mathrm{Tr}\sum_{\vec{s}_1,\vec{s}_2,\ldots,\vec{s}_{n-1}} H(\vec{s},\vec{s}_{n-1})\cdots H(\vec{s}_2,\vec{s}_1)H(\vec{s}_1,\vec{s}) \\ &= \sum_{\alpha} P_n(\alpha,j,\vec{s};\alpha,j,\vec{s}),\quad \vec{s}\in\Gamma_j,\end{aligned} \tag{12}$$

where the last equality was obtained with the help of Eq. (2) and the identification $H(\vec{s},\vec{s}\,')\equiv p(\vec{s},\vec{s}\,')$. The moment method requires, therefore, the computation of all possible closed walks, whereas, the Green's-function method, by making use of the periodicity of the crystal, performs this enumeration automatically, e.g., by calculating the integral in Eq. (7).

B. Local properties

The preceding results can be used as a basis for the analysis of vacancy defects or surfaces in the crystal. In random-walk language, these defects constitute a set of sites acting as permanant traps for the walker. By means of these traps we eliminate those walks, included in the generating function $P(\vec{s},\vec{s}\,';z)$ for the perfect crystal, that are no longer possible in the presence of defects.

Thus, let us suppose that (irreversible) traps exist at the set of q sites $Q=\{\vec{s}_1,\ldots,\vec{s}_q\}$ and let $Q_n(\vec{s},\vec{s}\,')$, $\vec{s},\vec{s}\,'\notin Q$ be the probability that a walker which starts to walk at site $\vec{s}\,'$ arrives at $\vec{s}$ at the nth step. In order to relate the $\{Q_n(\vec{s},\vec{s}\,')\}$ to the $\{P_n(\vec{s},\vec{s}\,')\}$ we find it useful to introduce yet another set of probabilities which we denote by $\{F_n(\vec{s}_l,\vec{s}\,')\}$. $F_n(\vec{s}_l,\vec{s}\,')$ is the probability that a walker, on the perfect lattice, starting from $\vec{s}\,'$ and avoiding the sites $\vec{s}_m\in Q$, $m\neq l$ reaches site $\vec{s}_l$ for the first time at the nth step. Both quantities $Q_n(\vec{s},\vec{s}\,')$ and $F_n(\vec{s}_l,\vec{s}\,')$ are to be understood as supermatrices with elements similar to those for $P_n(\vec{s},\vec{s}\,')$. The $\{F_n(\vec{s}_l,\vec{s}\,')\}$ satisfy the set of equations

$$\sum_{m=1}^{q}\sum_{k_m=1}^{n} P_{n-k_m}(\vec{s}_l,\vec{s}_m)F_{k_m}(\vec{s}_m,\vec{s}) = P_n(\vec{s}_l,\vec{s}\,'),\quad 1\le l\le q\,. \tag{13}$$

Equations (13) merely state the fact that the family of n-step walks between $\vec{s}\,'$ and $\vec{s}_l$ $(1\le l\le q)$ that give rise to $P_n(\vec{s}_l,\vec{s}\,')$ can be separated into different groups according to which of the sites $\vec{s}_m\in Q$ is visited first. And similarly, by subtracting from $P_n(\vec{s},\vec{s}\,')$ those walks that would otherwise lead to trapping, we have

$$Q_n(\vec{s},\vec{s}\,') = P_n(\vec{s},\vec{s}\,') - \sum_{m=1}^{q}\sum_{k_m=1}^{n} P_{n-k_m}(\vec{s},\vec{s}_m)F_{k_m}(\vec{s}_m,\vec{s}\,')\,. \tag{14}$$

In terms of the generating functions

$$F(\vec{s}_l,\vec{s}\,';z) = \sum_{n=1}^{\infty} F_n(\vec{s}_l,\vec{s}\,')z^n \tag{15}$$

and

$$Q(\vec{s},\vec{s}\,';z) = \sum_{n=0}^{\infty} Q_n(\vec{s},\vec{s}\,')z^n\,, \tag{16}$$

Eqs. (13) and (14) transform into

$$\sum_{m=1}^{q} P(\vec{s}_l,\vec{s}_m;z)F(\vec{s}_m,\vec{s}\,';z) = P(\vec{s}_l,\vec{s}\,';z)\,,\quad 1\le l\le q \tag{17}$$

and

$$Q(\vec{s},\vec{s}\,';z) = P(\vec{s},\vec{s}\,';z) - \sum_{m=1}^{q} P(\vec{s},\vec{s}_m;z)F(\vec{s}_m,\vec{s}\,';z)\,. \tag{18}$$

The resolution of the linear system (17) for the $F(\vec{s}_m,\vec{s}\,';z)$ yields the desired expression for $Q(\vec{s},\vec{s}\,';z)$ in terms of the basic function $P(\vec{s},\vec{s}\,';z)$. In particular, for the special case of one trap, we obtain

$$Q(\vec{s},\vec{s}\,';z) = P(\vec{s},\vec{s}\,';z) - P(\vec{s},\vec{s}_1;z)[P(\vec{s}_1,\vec{s}_1;z)]^{-1}P(\vec{s}_1,\vec{s}\,';z)\,. \tag{19}$$

Solving Eqs. (17) and (18) for arbitrary sets of traps becomes increasingly difficult for larger numbers of traps. An exception is the case when the traps constitute lines or planes of traps, for then, as we shall see in the following sections, Fourier-transformation techniques simplify the problem considerably.

The local density of states for the perturbed crystal we have considered is given by

$$D_j(\vec{s};E) = -\pi^{-1}\mathrm{Im}E^{-1}\sum_{\alpha} Q(\alpha,j,\vec{s};\alpha,j,\vec{s};E^{-1}),\quad \vec{s}\in\Gamma_j\,. \tag{20}$$

III. SURFACES

In this section we derive the Green's function appropriate to the surface of a semi-infinite crystal. We form the semi-infinite (cleaved) crystal by introducing a set of N contiguous planes of traps into the perfect-lattice framework. The function of these traps is to confine the walker within one semi-infinite region. Therefore, the necessary number of planes in the slab of traps is given by the range of the Hamiltonian. For the (100) surface of a sc crystal, a single plane is sufficient to deal with interactions up to third nearest neighbors. For other surfaces on the same sc crystal or for the same (100) surface on either fcc or bcc crystals, more planes are necessary when the interactions reach beyond nearest neighbors.

For clarity of presentation we discuss interactions of arbitrary range only for the case of a surface along the [100] direction on the sc lattice framework. Thus, if we let the set of traps be

$$Q=\{(l_1,l_2,l_3)|0\leqslant l_1<N,\,-\infty<l_2,l_3<\infty\}\,,$$

Eqs. (17) and (19) read

$$\sum_{m_1=0}^{N-1}\sum_{m_2=-\infty}^{\infty}\sum_{m_3=-\infty}^{\infty}P(l_1-m_1,l_2-m_2,l_3-m_3;z)F(m_1,s_1',m_2-s_2',m_3-s_3';z)=P(l_1-s_1',l_2-s_2',l_3-s_3';z)\,,\qquad 0\leqslant l_1<N,\quad -\infty<l_2,l_3<\infty \tag{21}$$

and

$$Q(s_1,s_1',s_2-s_2',s_3-s_3';z)=P(s_1-s_1',s_2-s_2',s_3-s_3';z)-\sum_{l_1=0}^{N-1}\sum_{l_2=-\infty}^{\infty}\sum_{l_3=-\infty}^{\infty}P(s_1-l_1,s_2-l_2,s_3-l_3;z)\times F(l_1,s_1',l_2-s_2',l_3-s_3';z)\,, \tag{22}$$

where $\vec{s}\,'=(s_1',s_2',s_3')$ and $\vec{s}=(s_1,s_2,s_3)$. The convolutions appearing in these equations suggest the introduction of the partial Fourier transformations

$$u_\kappa(s_1-s_1';z)=\sum_{\sigma}P(s_1-s_1',\sigma-\sigma';z)e^{i\vec{\kappa}\cdot\vec{\sigma}}\,, \tag{23a}$$

$$v_\kappa(s_1,s_1';z)=\sum_{\sigma}Q(s_1,s_1',\sigma-\sigma';z)e^{i\vec{\kappa}\cdot\vec{\sigma}}\,, \tag{23b}$$

and

$$w_\kappa(s_1,s_1';z)=\sum_{\sigma}F(s_1,s_1';\sigma-\sigma';z)e^{i\vec{\kappa}\cdot\vec{\sigma}}\,, \tag{23c}$$

where $\vec{\sigma}=(s_2,s_3)$ and $\vec{\kappa}=(k_2,k_3)$, and by means of which Eqs. (21) and (22) become

$$\sum_{l_1'=0}^{N-1}u_{\vec{\kappa}}(l_1-l_1';z)w_\kappa(l_1',s_1';z)=u_\kappa(l_1-s_1';z)\,,\quad 0\leqslant l_1<N \tag{24}$$

and

$$v_{\vec{\kappa}}(s_1,s_1';z)=u_{\vec{\kappa}}(s_1-s_1';z)-\sum_{l_1=0}^{N-1}u_{\vec{\kappa}}(s_1-l_1;z)w_{\vec{\kappa}}(l_1,s_1';z)\,. \tag{25}$$

By comparing Eqs. (24) and (25) with Eqs. (17) and (18), we observe that the three-dimensional problem with a slab of N trapping planes has been reduced in the transformed κ space into a one-dimensional problem of N contiguous traps. In particular, when one has one plane ($l_1=0$) and three planes ($l_1=-1,0,1$) of traps, we obtain, respectively,

$$v(s_1,s_1')=u(s_1-s_1')-u(s_1)u^{-1}(0)u(-s_1') \tag{26}$$

and

$$\begin{aligned}v(s_1,s_1')=&\,u(s_1-s_1')-u(s_1)u^{-1}(0)u(-s_1')\\&-[u(s_1-1)-u(s_1)u^{-1}(0)u(-1)][u(0)-u(1)u^{-1}(0)u(-1)]^{-1}[u(1-s_1')-u(1)u^{-1}(0)u(-s_1')]\\&-\{u(s_1+1)-u(s_1)u^{-1}(0)u(1)-[u(s_1-1)-u(s_1)u^{-1}(0)u(-1)][u(0)-u(1)u^{-1}(0)u(-1)]^{-1}\\&\qquad\times[u(2)-u(1)u^{-1}(0)u(1)]\}\\&\times\{u(0)-u(-1)u^{-1}(0)u(1)-[u(-2)-u(-1)u^{-1}(0)u(-1)][u(0)-u(1)u^{-1}(0)u(-1)]^{-1}[u(2)-u(1)u^{-1}(0)u(1)]\}^{-1}\\&\times\{u(-1-s_1')-u(-1)u^{-1}(0)u(-s_1')-[u(-2)-u(-1)u^{-1}(0)u(-1)][u(0)-u(1)u^{-1}(0)u(-1)]^{-1}\\&\qquad\times[u(1-s_1')-u(1)u^{-1}(0)u(-s_1')]\}\,,\end{aligned} \tag{27}$$

where we have omitted the subscript κ and z. The expressions above can be further simplified if the planes of traps effectively confine the walker to one region and if the regions are mirror images of each other with respect to the cleavage plane. In this case $v(s_1, s_1') = 0$ when $s_1 > 0$ and $s_1' < 0$, $u(s_1) = u(-s_1)$, and Eqs. (26) and (27) reduce, respectively, to

$$v(s_1, s_1') = u(s_1 - s_1') - u(s_1 + s_1'), \quad s_1, s_1' > 0 \tag{28}$$

and

$$v(s_1, s_1') = u(s_1 - s_1') - u(s_1 + s_1') - [u(s_1 - 1) - u(s_1 + 1)][u(0) - u(2)]^{-1}[u(s_1' - 1) - u(s_1' + 1)], \quad s_1, s_1' > 1. \tag{29}$$

Equation (28) can be integrated immediately to yield

$$Q(s_1, s_1', \vec{\sigma} - \vec{\sigma}'; z) = P(s_1 - s_1', \vec{\sigma} - \vec{\sigma}'; z) - P(s_1 + s_1', \vec{\sigma} - \vec{\sigma}'; z), \quad s_1, s_1' > 0. \tag{30}$$

This remarkably simple result which expresses the surface Green's function as the difference of two bulk Green's functions has been obtained previously for the special cases of a one-band sc crystal by Dobrzynsky and Mills[10] and for a two-band CsCl-type crystal with one orbital per atom by Ho *et al.*[2] As is clear from our derivation, this result only depends on the range of the interactions and on the symmetry properties of the cleavage plane. It is independent of both the number of interacting orbitals and the kinds of atoms which constitute the crystal.

According to Eqs. (6) and (7), Eq. (30) can be expressed as

$$Q(s_1, s_1', \vec{\sigma} - \vec{\sigma}'; z) = \frac{1}{(2\pi)^3} \int_0^{2\pi} \int_0^{2\pi} \int_0^{2\pi} d\kappa \, dk_1 \, e^{-i\vec{\kappa} \cdot (\vec{\sigma} - \vec{\sigma}')} \left(e^{-ik_1(s_1 - s_1')} - e^{-ik_1(s_1 + s_1')}\right) U(\mathrm{k}; z), \quad s_1, s_1' > 0 \tag{31a}$$

or, provided the walks are symmetrical in the s_1 direction, that is, $p(s_1, \vec{\sigma}) = p(-s_1, \vec{\sigma})$, for then $U(k_1, \vec{\kappa}; z) = U(-k_1, \vec{\kappa}; z)$, we have

$$Q(s_1, s_1', \vec{\sigma} - \vec{\sigma}'; z) = \frac{1}{2\pi^3} \int_0^{2\pi} \int_0^{2\pi} d\vec{\mathrm{k}} \int_0^{\pi} dk_1 \, e^{-i\vec{\kappa} \cdot (\vec{\sigma} - \vec{\sigma}')} \sin k_1 s_1 \sin k_1 s_1' U(\vec{\mathrm{k}}; z), \quad s_1, s_1' > 0. \tag{31b}$$

This last equation indicates that the eigenfunctions associated with the semi-infinite crystal are of the form $|\phi_{\vec{k}}(\vec{s})\rangle \sim e^{-i\vec{\kappa} \cdot \vec{\sigma}} \sin k_1 s_1$, and clearly reflect the boundary conditions imposed on the system.

We now turn our attention to the (110) and (111) surfaces when formed by one plane of traps. We find it convenient to embed our original sc lattice framework into a larger lattice in such a manner that the surface is of the (100) type (with as-sociated SBZ of square or rectangular shape) for the new lattice. The additional sites involved are empty and if the Hamiltonian is properly rescaled the problem remains unchanged. We illustrate the procedure in Figs. 2 and 3 for the (110) and (111) surfaces, for which the new coordinates can be chosen to be, respectively,

$$S_1 = \tfrac{1}{2}(s_1 + s_2), \quad S_2 = \tfrac{1}{2}(s_2 - s_1), \quad S_3 = s_3 \tag{32a}$$

and

$$S_1 = \tfrac{1}{3}(s_1 + s_2 + s_3), \quad S_2 = \tfrac{1}{2}(s_1 - s_2), \quad S_3 = \tfrac{1}{6}(s_1 + s_2 - 2s_3). \tag{32b}$$

It is clear that Eq. (26) holds true for the new reference system, i.e.,

$$v_{\vec{\mathrm{K}}}(S_1, S_1'; z) = u_{\vec{\mathrm{K}}}(S_1 - S_1'; z) - u_{\vec{\mathrm{K}}}(S_1; z)[u_{\vec{\mathrm{K}}}(0; z)]^{-1} u_{\vec{\mathrm{K}}}(-S_1'; z), \tag{33}$$

and thus the desired surface Green's functions can be obtained by first performing the inverse Fourier transformation of Eq. (33) and then re-ferring the resulting expression of the original coordinate system.

The cleavage plane for the (110) surface of the

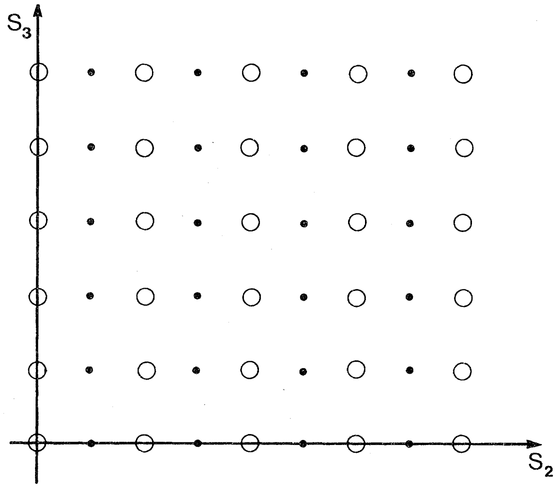

FIG. 2. Embedding of the sc lattice framework into a larger lattice for the analysis of (110) surfaces. We only show a layer of sites parallel to this surface and the dots are the additional empty sites.

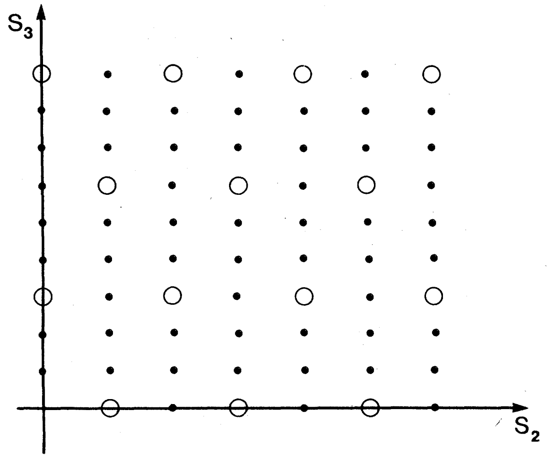

FIG. 3. Same as Fig. 2, but for (111) surfaces.

cubic crystals is again a plane of symmetry, and we have in this case that

$$Q(s_1, s_1', s_2, s_2', s_3 - s_3'; z) = P(s_1 - s_1', s_2 - s_2', s_3 - s_3'; z) - P(s_1 + s_2', s_2 + s_1', s_3 - s_3'; z), \quad s_1 + s_2', s_2 + s_1' > 0. \tag{34}$$

On the contrary, the (111) surface of the cubic crystals is not formed on a plane of symmetry and Eq. (28) is not applicable. To analyze further this type of surface we recall that for the perfect, translationally invariant, lattice framework we have

$$P(\vec{S}; z) - z \sum_{\vec{S}'} p(\vec{S} - \vec{S}')P(\vec{S}'; z) = \delta_{\vec{S},\vec{0}} I, \tag{35}$$

which, in the partial Fourier space we have employed, becomes

$$u_{\vec{K}}(S_1; z) - z \sum_{S_1'} \lambda_{\vec{K}}(S_1 - S_1')u_{\vec{K}}(S_1'; z) = \delta_{S_1,0} I, \tag{36}$$

where

$$\lambda_{\vec{K}}(S_1) = \sum_{\vec{\Sigma}} p(s_1, \vec{\Sigma})e^{-i\vec{K}\cdot\vec{\Sigma}}. \tag{37}$$

For interactions which vanish beyond nearest neighbors in the S_1 direction, Eq. (36) becomes

$$[I - z\lambda_{\vec{K}}(0)]u_{\vec{K}}(S_1; z) - z\lambda_{\vec{K}}(-1)u_{\vec{K}}(S_1 + 1; z) - z\lambda_{\vec{K}}(1)u_{\vec{K}}(S_1 - 1; z) = \delta_{S_1,0} I, \tag{38}$$

and since

$$v_{\vec{K}}(S_1, -S_1'; z) = 0 = u_{\vec{K}}(S_1 + S_1'; z) - u_{\vec{K}}(S_1; z)[u_{\vec{K}}(0; z)]^{-1}u_{\vec{K}}(S_1'; z), \quad S_1, S_1' > 0, \tag{39}$$

we conclude that

$$u_{\vec{K}}(S_1; z) = \{u_{\vec{K}}(1; z)[u_{\vec{K}}(0; z)]^{-1}\}^{S_1} u_{\vec{K}}(0; z), \quad S_1 > 0 \tag{40a}$$

and

$$u_{\vec{K}}(-S_1; z) = \{u_{\vec{K}}(-1; z)[u_{\vec{K}}(0; z)]^{-1}\}^{S_1} u_{\vec{K}}(0; z), \quad S_1 > 0. \tag{40b}$$

Thus, if we let

$$A_{\vec{K}} = u_{\vec{K}}(1; z)[u_{\vec{K}}(0; z)]^{-1} \tag{41a}$$

and

$$B_{\vec{K}} = u_{\vec{K}}(-1; z)[u_{\vec{K}}(0; z)]^{-1}, \tag{41b}$$

the recurrence relation (38) yields, for $S_1 = 0$, $S_1 = -1$, and $S_1 = 1$, the expressions

$$[I - z\lambda_{\vec{K}}(0)]u_{\vec{K}}(0; z) = I + z\lambda_{\vec{K}}(1)B_{\vec{K}}u_{\vec{K}}(0; z) + z\lambda_{\vec{K}}(-1)A_{\vec{K}}u_{\vec{K}}(0; z), \tag{42a}$$

$$[I - z\lambda_{\vec{K}}(0)]A_{\vec{K}} = z\lambda_{\vec{K}}(1) + z\lambda_{\vec{K}}(-1)A_{\vec{K}}^2 \tag{42b}$$

and

$$[I - z\lambda_{\vec{K}}(0)]B_{\vec{K}} = z\lambda_{\vec{K}}(1)B_{\vec{K}}^2 + z\lambda_{\vec{K}}(-1), \tag{42c}$$

respectively, from which we obtain

$$\lambda_{\vec{K}}(1)A_{\vec{K}}^{-1} + \lambda_{\vec{K}}(-1)A_{\vec{K}} = \lambda_{\vec{K}}(1)B_{\vec{K}} + \lambda_{\vec{K}}(-1)B_{\vec{K}}^{-1}. \tag{43}$$

Furthermore, if we restrict the discussion to the case when the interactions between each pair of nearest neighbors have the same strength, the quantities $\lambda_{\vec{K}}(\pm 1)$ are of the form $\lambda_{\vec{K}}(1) = \alpha_1 T$ and $\lambda_{\vec{K}}(-1) = \alpha_{-1} T$, with α_1 and α_{-1} scalars, and we find from Eq. (43) that

$$A_{\vec{K}} = \alpha_1 \alpha_{-1}^{-1} B_{\vec{K}}. \tag{44}$$

Now, since the walks on the perfect lattice are not biased towards any specific direction, from Eqs. (40), (41), and (44) we conclude that $|\alpha_1 \alpha_{-1}^{-1}|$ is necessarily unity, and hence $\alpha_1 \alpha_{-1}^{-1}$ represents only a phase factor. There is another solution to Eq. (43), namely, $A_{\vec{K}} = B_{\vec{K}}^{-1}$, but it does not satisfy the boundary condition $P_n(\vec{s}) \to 0$ when $|\vec{s}| \to \infty$, which in turn implies $u_{\vec{K}}(\pm S_1; z) \to 0$ as $S_1 \to \infty$.

Finally, through the employment of Eqs. (40), (41), and (44), together with Eqs. (23) and (6), Eq. (39) is transformed into

$$Q(S_1,S_1',\vec{\Sigma}-\vec{\Sigma}';z)=\frac{1}{(2\pi)^3}\int_0^{2\pi}\int_0^{2\pi}\int_0^{2\pi}d\vec{K}\,e^{-i\vec{K}\cdot(\vec{\Sigma}-\vec{\Sigma}')}\tfrac{1}{2}[e^{-iK_1S_1}-(\alpha_1\alpha_{-1}^{-1})^{S_1}e^{iK_1S_1}]$$
$$\times[e^{iK_1S_1'}-(\alpha_{-1}\alpha_1^{-1})^{S_1'}e^{-iK_1S_1'}]U(\vec{K};z),\qquad S_1>S_1'>0. \tag{45}$$

The expression above is a generalization of Eq. (31), and reduces to it when the surface is a plane of symmetry, for then $\alpha_1\alpha_{-1}^{1}=1$. Also, we observe that the eigenfunctions have the form

$$|\phi_{\vec{K}}(\vec{S})\rangle\sim e^{-i\vec{K}\cdot\vec{\Sigma}}[e^{-iK_1S_1}-(\alpha_1\alpha_{-1}^{-1})^{S_1}e^{iK_1S_1}].$$

For the particular case of a (111) surface on a sc crystal one has

$$\alpha_1=e^{i(K_2+K_3)}+e^{-i(K_2-K_3)}+e^{-2iK_3}, \tag{46}$$

with $\alpha_{-1}=\alpha_1^*$.

As an example of the preceding, we present calculations for a model of rocksalt made up of two interwoven fcc sublattices (denoted by Γ_1 and Γ_2) and one orbital per site. Each orbital interacts only with its nearest neighbors. In this case

$$\Lambda(\vec{k})=\begin{bmatrix}\epsilon_1 & t\lambda(\vec{k})\\ t\lambda(\vec{k}) & \epsilon_2\end{bmatrix},$$

where ϵ_1 and ϵ_2 are the electronic energies, t is the two-center hopping integral, and

$$\lambda(\vec{k})=2(\cos k_1+\cos k_2+\cos k_3).$$

For the generating function $P(\vec{s};z)$ we obtain

$$P(\vec{s};z)=P^{(0)}(\vec{s};\zeta)\begin{pmatrix}(1-z\epsilon_1)^{-1}\Delta(\vec{s}) & [(1-z\epsilon_1)(1-z\epsilon_2)]^{-1/2}[1-\Delta(\vec{s})]\\ [(1-z\epsilon_1)(1-z\epsilon_2)]^{-1/2}[1-\Delta(\vec{s})] & (1-z\epsilon_2)^{-1}\Delta(\vec{s})\end{pmatrix}, \tag{47}$$

where $\Delta(\vec{s})=1$ when $\vec{s}$ connects two sites on the same sublattice and vanishes otherwise, and

$$P^{(0)}(\vec{s};\zeta)=\frac{1}{(2\pi)^3}\int_0^{2\pi}\int_0^{2\pi}\int_0^{2\pi}\frac{e^{-\vec{k}\circ\vec{s}}\,d\vec{k}}{1-\zeta\lambda(\vec{k})} \tag{48}$$

is the Green's function for the infinite, one-band sc crystal with nearest-neighbor interactions, where

$$\zeta=[(1-z\epsilon_1)(1-z\epsilon_2)]^{-1/2}zt. \tag{49}$$

In deriving Eq. (47) we have used the following property of nearest-neighbor walks on the two sublattice structures we are considering: Any two sites on the same sublattice may be connected only by walks having an even number of steps, whereas two sites on different sublattices are connected with an odd number of steps. Therefore, $P^{(0)}(\vec{s}-\vec{s}';\zeta)$ is a series in even powers of ζ when $\vec{s}$ and $\vec{s}'$ belong to the same sublattice and a series in odd powers of ζ otherwise, and thus

$$P^{(0)}(\vec{s}-\vec{s}';\zeta)=P^{(0)}(\vec{s}-\vec{s}';-\zeta),$$
$$\vec{s},\vec{s}'\in\Gamma_1 \text{ or } \vec{s},\vec{s}'\in\Gamma_2 \tag{50a}$$

and

$$P^{(0)}(\vec{s}-\vec{s}';\zeta)=-P^{(0)}(\vec{s}-\vec{s}';-\zeta),$$
$$\vec{s}\in\Gamma_1 \text{ and } \vec{s}'\in\Gamma_2 \text{ or } \vec{s}'\in\Gamma_2 \text{ and } \vec{s}'\in\Gamma_1. \tag{50b}$$

The employment of Eqs. (7), (9), (46), and (50), together with

$$[1-\zeta^2\lambda^2(k)]^{-1}=\tfrac{1}{2}\{[1-\zeta\lambda(k)]^{-1}+[1+\zeta\lambda(k)]^{-1}\} \tag{51a}$$

and

$$\zeta\lambda(k)[1-\zeta^2\lambda^2(k)]^{-1}=\tfrac{1}{2}\{[1-\zeta\lambda(k)]^{-1}-[1+\zeta\lambda(k)]^{-1}\} \tag{51b}$$

leads to (47).

In Figs. 4–6 we show the local density of states (LDOS) per atom for the first few layers of the (100), (110), and (111) surfaces and compare them with the bulk density of states. Our choice of parameters was $\epsilon_1=-\epsilon_2=2$ in units of t. All curves show the band-gap characteristic of binary crystals with only nearest-neighbor interactions, its width being determined by 2ϵ. This width will narrow for extended interactions as found in Ref. 2. For the (100) and (110) surfaces we calculated numerically the integral representation[18]

$$\mathrm{Im}P^{(0)}(s_1,0,0;\zeta)=\frac{1}{2\pi^2\zeta}\int_0^{\min[\pi,\cos^{-1}(1/2\zeta-2)]}dk_1\cos s_1k_1K\left(\frac{(q-1)^{1/2}}{q}\right), \tag{52}$$

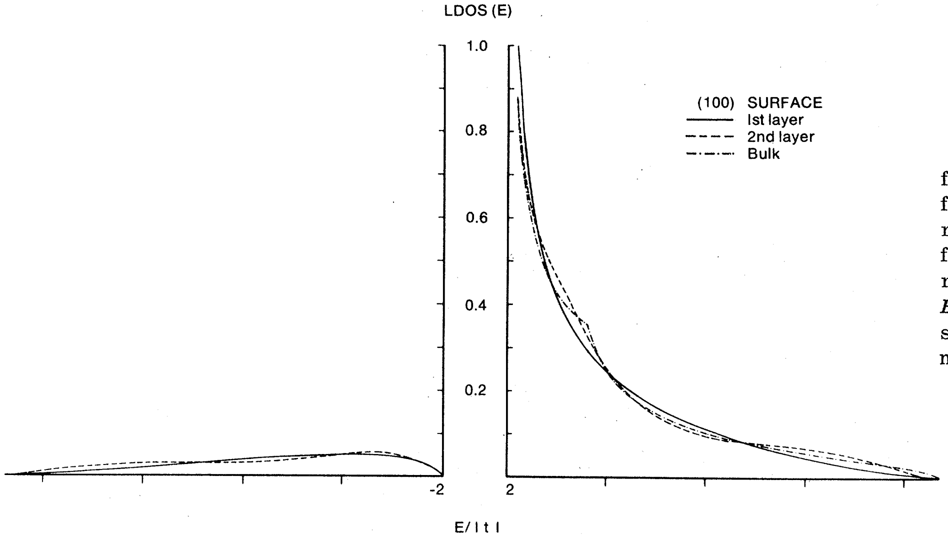

FIG. 4. LDOS for the first few layers of the (100) surface for type II atoms of the rocksalt model. The LDOS for type I atoms is the mirror image with respect to $E=0$. The bulk density of states in the $E<0$ region is not drawn for clarity.

with

$$q=4\xi(1-2\xi\cos k_1)^{-1}$$

and K being the complete elliptic integral of the first kind for the one-band sc crystal and subsequently employed it in Eqs. (47), (30), (34), and (20). Each layer parallel to these surfaces contains the two types of atoms (I and II) of the crystal. From the form of the surface Green's functions [Eq. (47) together with (30) or (34)] the LDOS for I atoms is the mirror image, with respect to our zero of energy, of that for II atoms. The LDOS for the (111) surface was calculated by sampling the surface Brillouin zone and integrating numerically Eq. (33). In this case the layers of atoms parallel to the surface have only one kind of atom each; we chose the first layer to be of type I. Thus in Fig. 6(a) we show the LDOS for the first and third layers and in Fig. 6(b) that for the second and fourth layers. For all the surfaces we observe that the LDOS at the surface shows a narrowing in energy compared with that of the bulk, similar to that found by Ho *et al.*[2] in their CsCl crystal model. This effect is less noticeable in the (100) surface, but becomes more pronounced for the (110) case and even more for the (111) surface. This behavior can be understood when we recall that the number of bonds per atom broken to form the surface is one, two, and three for the [100], [110], and [111] directions, respectively.

IV. THIN FILMS

To calculate the Green's function for a thin-film structure we introduce two parallel slabs

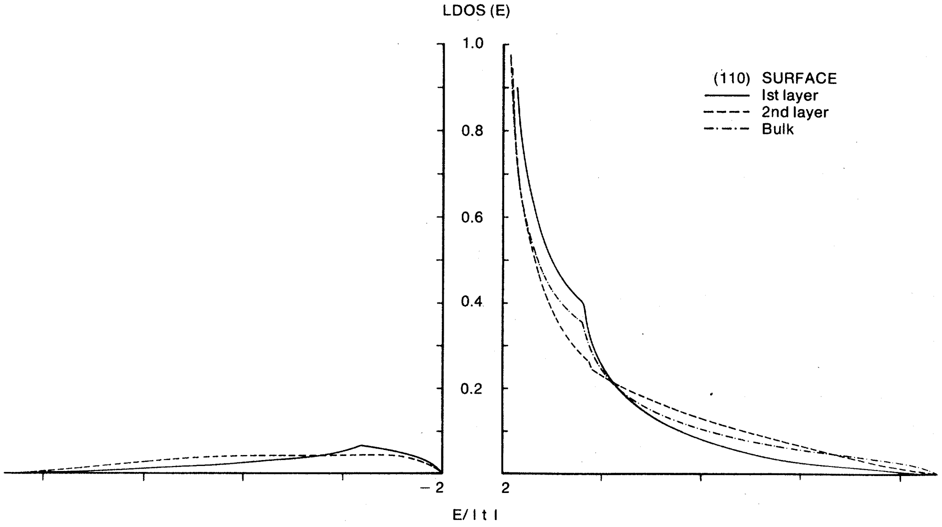

FIG. 5. The same as Fig. 4, but for the (110) surface.

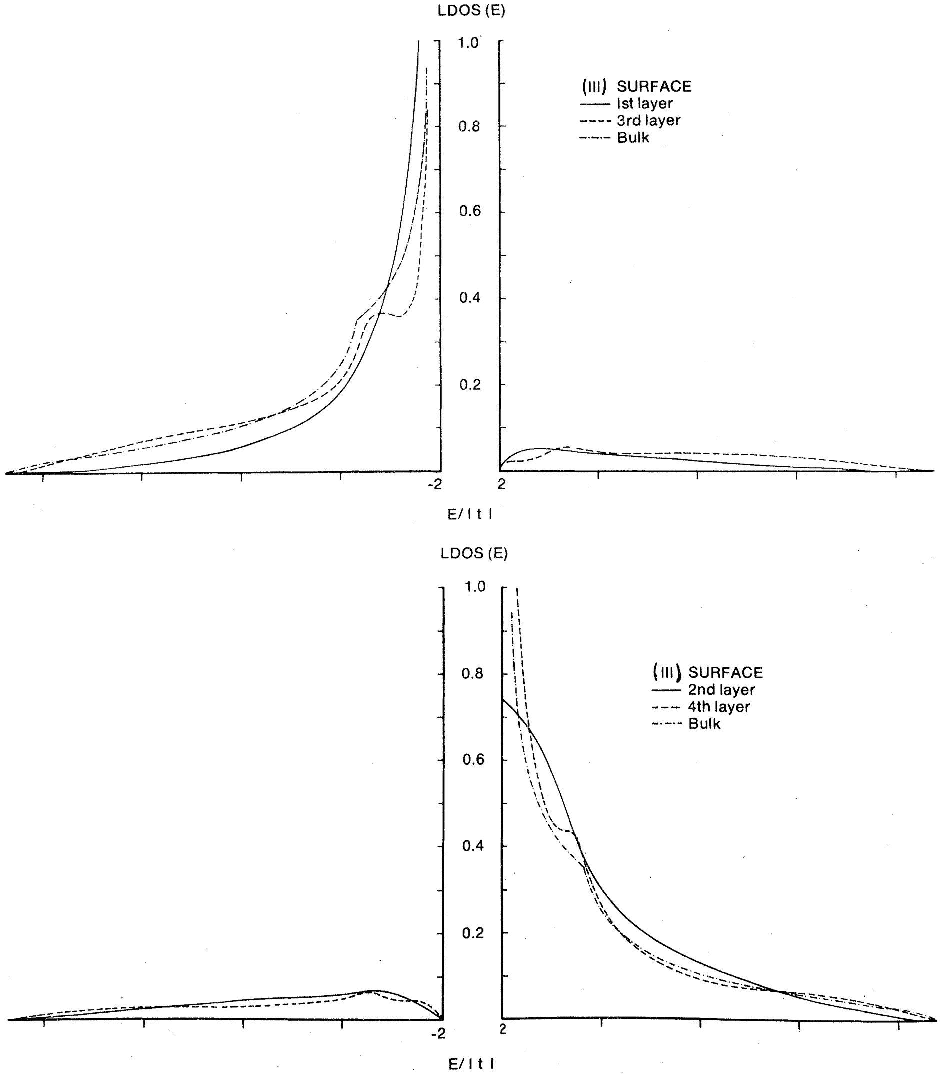

FIG. 6. LDOS for the first few layers of the (111) surface of the rocksalt model: (a) Layers of the type-I atoms; (b) layers of type-II atoms.

of planes of traps into the infinite lattice framework. It is clear that the derivation of the basic set of equations for this problem is the same as that for the one-surface problem, and that it is only necessary to extend the summations in Eqs. (24) and (25) to the two slabs of traps. When the film is formed only by the planes $(0, l_2, l_3)$ and (L, l_2, l_3), we have

$$v(s_1,s_1')=u(s_1-s_1')-u(s_1)u^{-1}(0)u(-s_1') - [u(s_1-L)-u(s_1)u^{-1}(0)u(-L)][u(0)-u(L)u^{-1}(0)u(-L)]^{-1}[u(L-s_1')-u(L)u^{-1}(0)u(-s_1')]. \quad (53)$$

And if we again assume the symmetry property $u(s_1)=u(-s_1)$, together with the condition that $v(s_1,s_1')=0$ if s_1 and s_1' correspond to sites on different sides of the planes of traps, we have

$$u(s_1+s_1')=u(s_1)u^{-1}(0)u(s_1')=u(s_1)u^{-1}(0)u(-s_1') \quad (54)$$

and thus

$$v(s_1,s_1')=u(s_1-s_1')-u(s_1+s_1')-[u(s_1-L)-u(s_1+L)][u(0)-u(2L)]^{-1}[u(L-s_1')-u(L+s_1')], \quad (55)$$

$$0<s_1,s_1'<L.$$

Furthermore, since [see Eq. (40)]

$$u(s_1)=u(0)[u^{-1}(0)u(1)]^{|s_1|}=[u(1)u^{-1}(0)]^{|s_1|}u(0)\,, \tag{56}$$

the last term in Eq. (55) can be expanded to yield

$$\begin{aligned} v(s_1,s_1')&=u(s_1-s_1')-u(s_1+s_1')\\ &\quad-\sum_{n=1}^{\infty}[u(2nL-s_1-s_1')-u(2nL-s_1+s_1')-u(2nL+s_1-s_1')+u(2nL+s_1+s_1')]\,,\; 0<s_1,s_1'<L\,, \end{aligned} \tag{57}$$

and hence we obtain, for the Green's function of a film of width L cut along the [100] direction, the expression

$$\begin{aligned} Q(s_1,s_1',\sigma-\sigma';z)&=P(s_1-s_1',\sigma-\sigma';z)-P(s_1+s_1',\sigma-\sigma';z)\\ &\quad-\sum_{n=1}^{\infty}[P(2nL-s_1-s_1',\sigma-\sigma';z)-P(2nL-s_1+s_1',\sigma-\sigma';z)\\ &\quad P(2nL+s_1-s_1',\sigma-\sigma';z)-P(2nL+s_1+s_1',\sigma-\sigma';z)]\,,\; 0<s_1,s_1'<L\,. \end{aligned} \tag{58}$$

If the equation above is employed to construct the LDOS for the film it becomes necessary to know explicitly the nondiagonal terms of the bulk Green's function. However, since this last function is expected to decrease rapidly as the distance between the two reference sites increases, only a few terms in the series above will make important contributions to the LDOS for moderately large L. An alternative form of Eq. (58), obtained by summing the series, proves to be more advantageous in actual calculations, particularly when the bulk Green's function is not available, as is often the case. Equation (58) can be expressed as [see Eqs. (6) and (7)] as

$$Q(s_1,s_1',\vec{\sigma}-\vec{\sigma}';z)=\frac{1}{(2\pi)^3}\int_0^{2\pi}\int_0^{2\pi}\int_0^{2\pi}dk_1\,d\vec{\kappa}\,e^{-i\vec{\kappa}\cdot(\vec{\sigma}-\vec{\sigma}')}U(\vec{\mathrm{k}};z)\lim_{M\to\infty}F_M(k_1)\,, \tag{59}$$

where

$$F_M(k_1)=e^{-ik_1(s_1-s_1')}-e^{-ik_1(s_1+s_1')}+i[\cos(s_1-s_1')-\cos(s_1+s_1')]e^{ik_1L}\frac{(1-e^{2ik_1LM})}{\sin k_1L}; \tag{60}$$

or, provided $U(k_1,\vec{\kappa};z)=U(-k_1,\vec{\kappa};z)$, as

$$Q(s_1,s_1',\vec{\sigma}-\vec{\sigma}';z)=\frac{1}{(2\pi)^3}\int_0^{2\pi}\int_0^{2\pi}d\vec{\kappa}\,e^{-i\vec{\kappa}\cdot(\vec{\sigma}-\vec{\sigma}')}\int_0^{\pi}dk_1\,U(\vec{\mathrm{k}};z)\lim_{M\to\infty}E_M(k_1)\,, \tag{61}$$

where

$$\begin{aligned} E_M(k_1)&=F_M(k_1)+F_M(-k_1)\\ &=4\sin k_1s_1\sin k_1s_1'\left(\cos 2k_1LM+\cos k_1L\frac{\sin 2k_1LM}{\sin k_1L}\right). \end{aligned} \tag{62}$$

As $M\to\infty$ the first term in the large parentheses above oscillates rapidly around $k_1=0$, and therefore it does not contribute to the integration in Eq. (61). The second term behaves like the interference function in Fraunhofer diffraction and thus we have

$$\lim_{M\to\infty}\frac{\sin 2k_1LM}{\sin k_1L}=\sum_{l=1}^{L-1}(-1)^n\frac{\pi}{L}\delta\left(k_1-\frac{l\pi}{L}\right). \tag{63}$$

Hence,

$$Q(s_1,s_1',\sigma-\sigma';z)=\frac{2}{L}\sum_{l=1}^{L-1}\sin\frac{l\pi s_1}{L}\sin\frac{l\pi s_1'}{L}\frac{1}{(2\pi)^2}\int_0^{2\pi}\int d\kappa\,e^{-i\vec{\kappa}\cdot(\vec{\sigma}-\vec{\sigma}')}U\left(\frac{l\pi}{L},\vec{\mathrm{k}};z\right). \tag{64}$$

It is interesting to note that the boundary conditions which define the film provide us with wave functions of the form

$$|\phi_{\vec{k}}(\vec{s})\rangle \sim e^{-i\vec{k}\cdot\vec{\sigma}}\sin\frac{l\pi s_1}{L}, \quad 0<l\leq L.$$

If these are compared with those we obtained for a semi-infinite crystal we find, not unexpectedly, that the introduction of a second plane of traps has the effect of quantizing the values for k_1 (i.e., we have imposed the boundary conditions for a one-dimensional box).

As an application of this formalism we now study a metal film represented by a two-band bcc structure. In this case the associated random-walk problem is chosen to have a structure function

$$\Lambda(\vec{k}) = \begin{bmatrix} \epsilon^s + t^{ss}\lambda(\vec{k}) & \gamma^{sd} \\ \gamma^{sd} & \epsilon^d + t^{dd}\lambda(\vec{k}) \end{bmatrix}, \tag{65}$$

where ϵ^s and ϵ^d are the energies for s- and d-type electrons, respectively, t^{ss} and t^{dd} are nearest-neighbor hopping integrals, γ^{sd} represents s-d hybridization, and

$$\lambda(\vec{k}) = 8\cos k_1 \cos k_2 \cos k_3$$

(Refs. 17). For the Fourier transform $U(\vec{k};z)$ of the generating function $P(\vec{s};z)$, we obtain

$$U(\vec{k};z) = [(1-z_{sd}^2)(\zeta_+ - \zeta_-)]^{-1} U^{(0)}(\vec{k};\zeta_+)\begin{bmatrix} a_+ & c\zeta_+ \\ c\zeta_+ & b_+ \end{bmatrix}$$

$$- U^{(0)}(\vec{k};\zeta_-)\begin{bmatrix} a_- & c\zeta_- \\ c\zeta_- & b_- \end{bmatrix}, \tag{66}$$

where

$$a_\pm = (1-z\epsilon^s)^{-1}(\zeta_\pm - z_d),$$

$$b_\pm = (1-z\epsilon^d)^{-1}(\zeta_\pm - z_d),$$

$$c = [(1-z\epsilon^s)(1-z\epsilon^d)]^{-1/2} z_{sd},$$

with

$$z_s = zt^{ss}/(1-z\epsilon^s), \tag{67a}$$

$$z_d = zt^{dd}/(1-z\epsilon^d), \tag{67b}$$

$$z_{sd}^2 = [(\gamma^{sd})^2/t^{ss}t^{dd}]z_s z_d, \tag{67c}$$

$$\zeta_\pm = [2z_s z_d(1-z_{sd}^2)]^{-1} \times\{z_s + z_d \pm [(z_s+z_d)^2 - 4z_s z_d(1-z_{sd}^2)]^{1/2}\}, \tag{67d}$$

and

$$U^{(0)}(\vec{k};\zeta_\pm) = [1-\zeta_\pm\lambda(\vec{k})]^{-1}, \tag{68}$$

which is the Green's function in $\vec{k}$ space for the infinite, one-band bcc crystal with nearest-neighbor interactions.

It is possible to obtain the density of states of our bcc film in closed analytical form. For it can be shown that[18]

$$\operatorname{Im}\frac{1}{(2\pi)^2}\int_0^{2\pi}\int_0^{2\pi} d\vec{\kappa}\, U^{(0)}\left(\frac{l\pi}{L},\vec{\kappa};\zeta\right) = \begin{cases} \operatorname{sgn}\left(\frac{\partial\zeta}{\partial z}\right)\left(4\pi\zeta\left|\cos\frac{l\pi}{L}\right|\right)^{-1} K((1-q^2)^{1/2}), & 0<q^2<1 \\ 0, \quad q^2>1 \end{cases} \tag{69}$$

where

$$q = |8\zeta\cos(l\pi/L)|^{-1},$$

K is the complete elliptic integral of the first kind, and ζ is given by Eq. (67d) when the energy E has a small positive imaginary part (i.e., $z^{-1}=E+i\epsilon$). Then, employment of Eq. (69) into Eqs. (66), (64), and (20) yields for the LDOS

$$D(s_1;E) = Az\left[\operatorname{sgn}\left(\frac{\partial\zeta_+}{\partial z}\right)B_+\sum_{l=1}^{L_+}\zeta_+^{-1}\frac{\sin^2(ls_1\pi/L)}{|\cos(\pi l/L)|}K((1-q_+^2)^{1/2})\right.$$

$$\left.-\operatorname{sgn}\left(\frac{\partial\zeta_-}{\partial z}\right)B_-\sum_{l=1}^{L_-}\zeta_-^{-1}\frac{\sin^2(ls_1\pi/L)}{|\cos(l\pi/L)|}K((1-q_-^2)^{1/2})\right], \tag{70}$$

with

$$A = [2\pi^2 L(1-z_{sd}^2)(\zeta_+ - \zeta_-)]^{-1},$$

$$B_\pm = [(1-z\epsilon^s)^{-1}(\zeta_\pm - z_d) + (1-z\epsilon^d)^{-1}(\zeta_\pm - z_s)],$$

and where the upper limits in the summations, $L_\pm$, are the larger integers satisfying the condition

$$|8\zeta_\pm\cos(l\pi/L_\pm)| > 1.$$

Furthermore, we observe from Eq. (70) that $D(s_1;E)$ diverges for those values of the energy for which q

vanishes, or equivalently, when $z_{sd}=1$. The energies at which this occurs are easily found to be given by

$$E=\tfrac{1}{2}\{(\epsilon^s+\epsilon^d)\pm[(\epsilon^s-\epsilon^d)^2+4(\gamma^{sd})^2]^{1/2}\}. \tag{71}$$

These singularities are nonessential since the elliptic function K diverges logarithmically when its argument approaches unity. Also, it is interesting to note that in case L is even, that is, when the film is made up of an odd number of layers, there are extra divergencies for the LDOS when s_1 is odd. These are δ functions, and appear located at the same energies given by Eq. (71). To see this, we consider the imaginary part of that term of the trace of Eq. (64) for which $l=\frac{1}{2}L$, $s_1=s_1'$, and $\sigma=\sigma'$. Taking into account Eqs. (66), (68), and (70), we have

$$\begin{aligned}\operatorname{Im}\frac{2}{L}\sin^2\frac{s_1\pi}{2}\frac{1}{(2\pi)^2}\int_0^{2\pi}\int_0^{2\pi}d\vec{\kappa}\,[U_{11}(\tfrac{1}{2}\pi,\vec{\kappa};z)+U_{22}(\tfrac{1}{2}\pi,\vec{\kappa};z)]\\
=\operatorname{Im}A\sin^2\frac{s_1\pi}{2}\sum_{+,-}(\pm)B_\pm\zeta_\pm^{-1}\lim_{\chi\to L/2}\lim_{z\to 0^+}\int_0^{2\pi}\int_0^{2\pi}dk_2\,dk_3\left(\frac{\zeta_\pm}{\zeta_\pm^2+z^2}-8\cos\frac{\chi\pi}{L}\cos k_2\cos k_3-\frac{iz}{\zeta_\pm^2+z^2}\right)^{-1}\\
=\pi A\sin^2\frac{s_1\pi}{2}\sum_{+,-}(\pm)B_\pm\zeta_\pm^{-1}\lim_{\chi\to L/2}\int_0^{2\pi}\int_0^{2\pi}dk_1\,dk_2\,\delta\left(\zeta_\pm^{-1}-8\cos\frac{\chi\pi}{L}\cos k_2\cos k_3\right)\\
=\pi A\sin^2\frac{s_1\pi}{2}\sum_{+,-}(\pm)B_\pm\zeta_\pm^{-1}\delta(\zeta_\pm^{-1}).\end{aligned} \tag{72}$$

Thus, we see that this term contributes to the LDOS only when s_1 is odd and when $\zeta_\pm\to\infty$, in this limit $z_{sd}=1$ and E satisfies Eq. (71).

In Fig. 7 we show the LDOS for the first, second, and fifth layers for a film of ten layers. The values chosen for the interaction parameters were $\epsilon^s=-\epsilon^d=1$, $t^d=-0.1$, and $\gamma^{sd}=-0.2$ in units of $|t^s|$. The three curves show the two-peak structure characteristic of s and d orbitals. The most interesting feature of the LDOS at the first layer, when compared with that at the center, is the depletion of the s peak at the expense of an increase of the density for the d peak. This situation is reversed for the second layer, and we found this alternate behavior to hold for subsequent layers. As a consequence of this, the density of

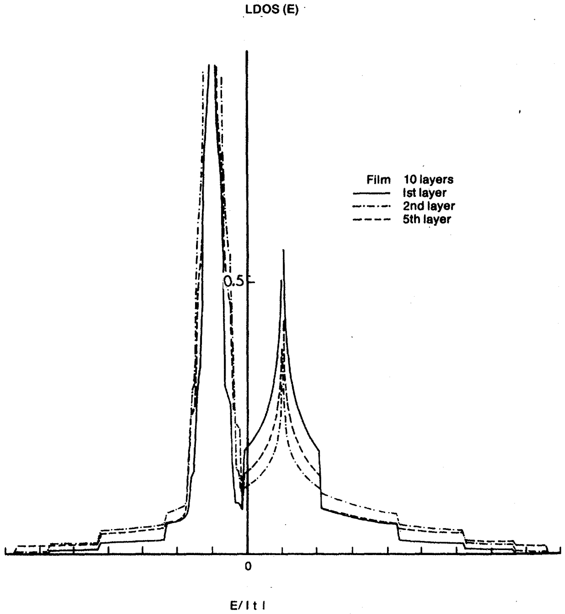

FIG. 7. LDOS for the first, second, and fifth layers for a film of ten layers with a two-band bcc structure.

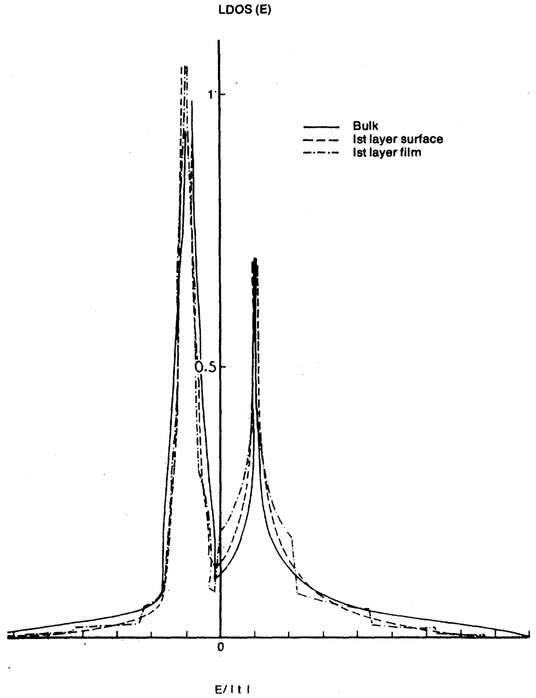

FIG. 8. Density of states for a two-band bcc structure: –·–·–·–, the first layer of a ten-layer film; – – – – –, the first layer of the semi-infinite system; ———, the infinite system.

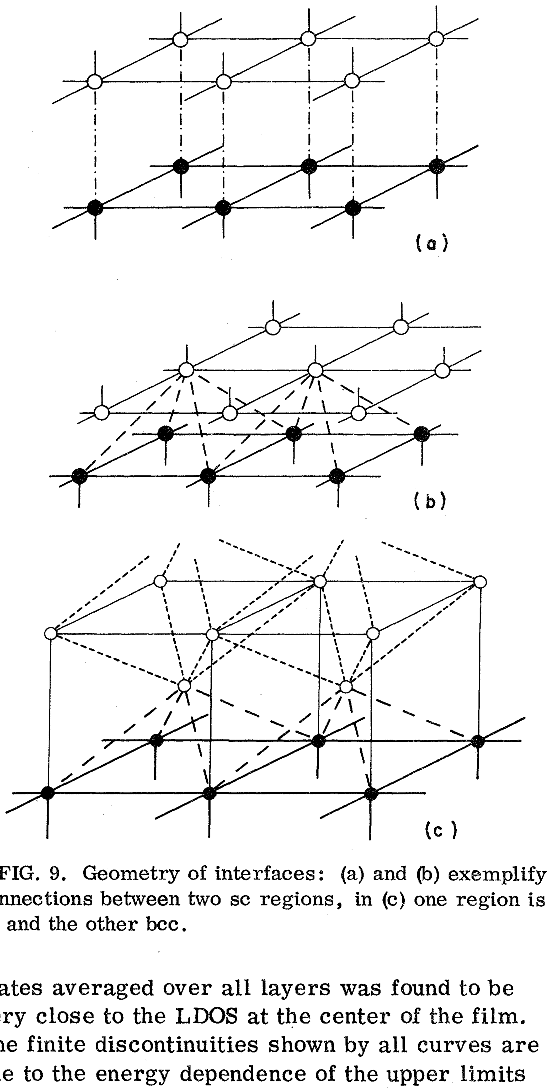

FIG. 9. Geometry of interfaces: (a) and (b) exemplify connections between two sc regions, in (c) one region is sc and the other bcc.

states averaged over all layers was found to be very close to the LDOS at the center of the film. The finite discontinuities shown by all curves are due to the energy dependence of the upper limits of the summations in Eq. (70). In Fig. 8 we compare the LDOS for the first layer of the ten-layer film with those for the surface of the semi-infinite crystal and for the bulk infinite system. Here we observe too, that the LDOS for the one-surface system (at its first layer), when compared with the bulk density, shows a depletion of the s peak and an increase of the d peak. This effect is even stronger at the surfaces of the film.

V. SOLID INTERFACES

Let us consider two semi-infinite crystals with (100) surfaces. The two crystals, denoted by a and b, may differ in chemical composition and lattice structure, but both are characterized by a sc lattice framework (as described in Sec. II) of the same lattice spacing. A planar interface is formed by connecting these two systems along their surfaces. The geometry of two different connections for two sc regions is shown in Figs. 9(a) and 9(b), whereas in Fig. 9(c) we show an interface between a sc and a bcc region.

We first introduce the matrices

$$\mathcal{J}_n(\vec{s},\vec{s}\,')=\begin{bmatrix} J_n^{aa}(\vec{s},\vec{s}\,') & J_n^{ab}(\vec{s},\vec{s}\,') \\ J_n^{ba}(\vec{s},\vec{s}\,') & J_n^{bb}(\vec{s},\vec{s}\,') \end{bmatrix} \tag{73}$$

and

$$\mathcal{p}(\vec{s},\vec{s}\,')=\begin{bmatrix} 0 & p^{ab}(\vec{s},\vec{s}\,') \\ p^{ba}(\vec{s},\vec{s}\,') & 0 \end{bmatrix}\,, \tag{74}$$

where $J_n^{\mu\nu}(\vec{s},\vec{s}\,')$ is the probability that a walker starting at $\vec{s}\,'$ in region ν arrives at $\vec{s}$ in region μ after the nth step, whereas $p^{\mu\nu}(\vec{s},\vec{s}\,')$ is the transition probability for a jump from one region to the other. For simplicity we specialize to the case where the $p^{\mu\nu}(\vec{s},\vec{s}\,')$ vanish if $\vec{s}$ and $\vec{s}\,'$ are not nearest neighbors. Both quantities, the $\{J_n^{\mu\nu}(\vec{s},\vec{s}\,')\}$ and the $\{p^{\mu\nu}(\vec{s},\vec{s}\,')\}$, are supermatrices with elements similar to those for $P_n(\vec{s},\vec{s}\,')$ and $p(\vec{s},\vec{s}\,')$. Now if we denote by $Q_n^a(s_1,s_1',\sigma-\sigma')$ and $Q_n^b(s_1,s_1',\sigma-\sigma')$ the probabilities for the n-step walks between sites $\vec{s}\,'=(s_1',\sigma')$ and $\vec{s}=(s_1,\sigma)$ which are confined to the regions a and b, respectively, we have that

$$J_n^{aa}(s_1,s_1',\sigma-\sigma')=Q_n^a(s_1,s_1',\sigma-\sigma')+\sum_{\substack{n_1,n_2,n_3\\(n_1+n_2+n_3+2=n)}}\;\sum_{\sigma_1,\ldots,\sigma_4}Q_{n_3}^a(s_1,1,\sigma-\sigma_4)p^{ab}(1,1,\sigma_4-\sigma_3)Q_{n_2}^b(1,1,\sigma_3-\sigma_2)$$
$$\times p^{ba}(1,1,\sigma_2-\sigma_1)Q_{n_1}^a(1,s_1',\sigma_1-\sigma')+\cdots \tag{75a}$$

and

$$J_n^{ab}(s_1,s_1',\sigma-\sigma')=\sum_{\substack{n_1,n_2\\(n_1+n_2+1=n)}}\;\sum_{\sigma_1,\sigma_2}Q_{n_2}^a(s_1,1,\sigma-\sigma_2)p^{ab}(1,1,\sigma_2-\sigma_1)Q_{n_1}^b(1,s_1',\sigma_1-\sigma')$$
$$+\sum_{\substack{n_1,\ldots,n_4\\(\Sigma_i^4 n_i+3=n)}}\;\sum_{\sigma_1,\ldots,\sigma_6}Q_{n_4}^a(s_1,1,\sigma-\sigma_6)p^{ab}(1,1,\sigma_6-\sigma_5)Q_{n_3}^b(1,1,\sigma_5-\sigma_4)p^{ba}(1,1,\sigma_4-\sigma_3)$$
$$\times Q_{n_2}^a(1,1,\sigma_3-\sigma_2)p^{ab}(1,1,\sigma_2-\sigma_1)Q_{n_1}^b(1,s_1',\sigma_1-\sigma')+\cdots\,, \tag{75b}$$

and similarly for J_n^{ba} and J_n^{bb}. In terms of the generating functions

$$J^{\mu\nu}(\vec{s},\vec{s}\,';z)=\sum_{n=0}^{\infty} J_n^{\mu\nu}(\vec{s},\vec{s}\,')z^n \tag{76a}$$

and

$$Q^{\mu}(\vec{s},\vec{s}\,';z)=\sum_{n=0}^{\infty} Q_n^{\mu}(\vec{s},\vec{s}\,')z^n\,, \tag{76b}$$

Eqs. (75) become

$$\begin{aligned}J^{aa}(s_1,s_1',\vec{\sigma}-\vec{\sigma}\,';z)=Q^a(s_1,s_1',\vec{\sigma}-\vec{\sigma}\,';z)+\sum_{\sigma_1,\ldots,\sigma_4} Q^a(s_1,1,\vec{\sigma}-\vec{\sigma}_4;z)p^{ab}(1,1,\vec{\sigma}_4-\vec{\sigma}_3)zQ^b(1,1,\vec{\sigma}_3-\vec{\sigma}_2;z)\\ \times p^{ba}(1,1,\vec{\sigma}_2-\vec{\sigma}_1)zQ^a(1,s_1',\vec{\sigma}_1-\vec{\sigma}\,';z)+\cdots\end{aligned} \tag{77a}$$

and

$$\begin{aligned}J^{ab}(s_1,s_1',\vec{\sigma}-\vec{\sigma}\,';z)=&\sum_{\sigma_1,\sigma_2} Q^a(s_1,1,\vec{\sigma}-\vec{\sigma}_2;z)p^{ab}(1,1,\vec{\sigma}_2-\vec{\sigma}_1)zQ^b(1,s_1',\vec{\sigma}_1-\vec{\sigma}\,';z)\\ &+\sum_{\sigma_1,\ldots,\sigma_6} Q^a(s_1,1,\vec{\sigma}-\vec{\sigma}_6,z)p^{ab}(1,1,\vec{\sigma}_6-\vec{\sigma}_5)zQ^b(1,1,\vec{\sigma}_5-\vec{\sigma}_4;z)p^{ba}(1,1,\vec{\sigma}_4-\vec{\sigma}_3)z\\ &\times Q^a(1,1,\vec{\sigma}_3-\vec{\sigma}_2;z)p^{ab}(1,1,\vec{\sigma}_2-\vec{\sigma}_1)zQ^b(1,s_1',\vec{\sigma}_1-\vec{\sigma}\,';z)+\cdots\,.\end{aligned} \tag{77b}$$

Finally, with the introduction of the partial Fourier transforms

$$\chi_{\vec{\kappa}}^{\mu\nu}(s_1,s_1';z)=\sum_{\sigma} J^{\mu\nu}(s_1,s_1',\sigma;z)e^{i\vec{\kappa}\cdot\vec{\sigma}}\,, \tag{78a}$$

$$\lambda_{\vec{\kappa}}^{\mu\nu}(1,1)=\sum_{\sigma} p^{\mu\nu}(1,1,\vec{\sigma})e^{i\vec{\kappa}\cdot\vec{\sigma}}\,, \tag{78b}$$

and

$$v_{\vec{\kappa}}^{\mu}(s_1,s_1';z)=\sum_{\sigma} Q^{\mu}(s_1,s_1',\vec{\sigma};z)e^{i\vec{\kappa}\cdot\vec{\sigma}}\,, \tag{78c}$$

Eqs. (77) reduce to

$$\begin{aligned}\chi_{\vec{\kappa}}^{aa}(s_1,s_1';z)=&v_{\vec{\kappa}}^{a}(s_1,s_1';z)+v_{\vec{\kappa}}^{a}(s_1,1;z)\lambda_{\vec{\kappa}}^{ab}(1,1)zv_{\vec{\kappa}}^{b}(1,1;z)\\ &\times[I-\lambda_{\vec{\kappa}}^{ba}(1,1)zv_{\vec{\kappa}}^{a}(1,1;z)\lambda_{\vec{\kappa}}^{ab}(1,1)zv_{\vec{\kappa}}^{b}(1,1;z)]^{-1}\lambda_{\vec{\kappa}}^{ba}(1,1)zv_{\vec{\kappa}}^{a}(1,s_1';z)\end{aligned} \tag{79a}$$

and

$$\chi_{\vec{\kappa}}^{ab}(s_1,s_1';z)=v_{\vec{\kappa}}^{a}(s_1,1;z)[I-\lambda_{\vec{\kappa}}^{ab}(1,1)zv_{\vec{\kappa}}^{b}(1,1;z)\lambda_{\vec{\kappa}}^{ba}(1,1)zv_{\vec{\kappa}}^{a}(1,1;z)]^{-1}\lambda_{\vec{\kappa}}^{ab}(1,1)zv_{\vec{\kappa}}^{b}(1,s_1';z)\,. \tag{79b}$$

It can be readily verified that Eqs. (79) satisfy the Dyson equation

$$\tilde{\chi}_{\vec{\kappa}}(s_1,s_1';z)=\tilde{v}_{\vec{\kappa}}(s_1,s_1';z)+\tilde{v}_{\vec{\kappa}}(s_1,1;z)\tilde{\lambda}_{\vec{\kappa}}(1,1)\tilde{\chi}_{\vec{\kappa}}(1,s_1';z)\,, \tag{80}$$

where

$$\tilde{\chi}_{\vec{\kappa}}=\begin{bmatrix}\chi_{\vec{\kappa}}^{aa} & \chi_{\vec{\kappa}}^{ab}\\ \chi_{\vec{\kappa}}^{ba} & \chi_{\vec{\kappa}}^{bb}\end{bmatrix}\,, \tag{81a}$$

$$\tilde{v}_{\vec{\kappa}}=\begin{bmatrix}v_{\vec{\kappa}}^{a} & 0\\ 0 & v_{\vec{\kappa}}^{b}\end{bmatrix}\,, \tag{81b}$$

and

$$\tilde{\lambda}_{\vec{\kappa}}=\begin{bmatrix}0 & \lambda_{\vec{\kappa}}^{ab}\\ \lambda_{\vec{\kappa}}^{ba} & 0\end{bmatrix}\,. \tag{81c}$$

Thus, to obtain the Green's function for the interface system we need to construct the coupling function $\tilde{\lambda}_{\vec{\kappa}}$ from the geometry of the connection and the interface interaction t. When one considers, for example, two regions of the same structure joined to form an otherwise perfect cubic crystal, we find

$$\lambda_{\vec{\kappa}}^{ab}(1,1)=\lambda_{\vec{\kappa}}^{ba}(1,1)=\begin{cases}t\,, & \text{sc}\\ 2t(\cos k_2+\cos k_3)\,, & \text{fcc}\\ 4t\cos k_2\cos k_3\,, & \text{bcc}\,.\end{cases} \tag{82}$$

The functions $v^a_{\vec\kappa}$ and $v^b_{\vec\kappa}$ can in turn be calculated from their respective bulk counterparts $u^a_{\vec\kappa}$ and $u^b_{\vec\kappa}$, as indicated in Sec. III.

For computational purposes we find it convenient to express Eq. (79a) in an alternative form. We shall restrict ourselves to interactions, in the bulk of the regions a and b, which vanish beyond nearest neighbors in the s_1 direction (that is, up to third, second, and first nearest neighbors for sc, fcc, and bcc crystals, respectively). We shall further assume that the interface is formed by surfaces which represent planes of symmetry of the respective perfect crystals. We obtain from Eqs. (40)–(42) with $A_\kappa = B_\kappa$ that

$$u_{\vec\kappa}(s_1;z) = A^{s_1}_{\vec\kappa}[z\lambda_{\vec\kappa}(1)(A^{-1}_{\vec\kappa} - A_{\vec\kappa})]^{-1}, \quad s_1 > 0 \tag{83}$$

and thus Eq. (28) can be written

$$v_{\vec\kappa}(s_1, s_1'; z) = A^{s_1 - s_1'}_{\vec\kappa} \sum_{r=0}^{s_1'-1} A^{2r+1}_{\vec\kappa} z^{-1} \lambda^{-1}_{\vec\kappa}(1), \qquad s_1 \geqslant s_1' > 0. \tag{84}$$

Finally, by substituting this last result into Eq. (79a), we obtain, after some manipulation, that

$$\chi^{aa}_{\vec\kappa}(s_1, s_1'; z) = z^{-1}\Big((A^a_{\vec\kappa})^{s_1 - s_1'} \sum_{r=0}^{s_1'-1} (A^a_{\vec\kappa})^{2r+1}[\lambda^a_{\vec\kappa}(1)]^{-1} + (A^a_{\vec\kappa})^{s_1}[\lambda^a_{\vec\kappa}(1)]^{-1}\lambda^{ab}_{\vec\kappa}|\,\lambda^{ab}_{\vec\kappa}(1,1)A^b_{\vec\kappa}[\lambda^b(1)]^{-1}$$
$$\times\{I - \lambda^{ba}_{\vec\kappa}(1,1)A^a_{\vec\kappa}[\lambda^a_{\vec\kappa}(1)]^{-1}\lambda^{ab}_{\vec\kappa}(1,1)A^b_{\vec\kappa}[\lambda^b_{\vec\kappa}(1)]^{-1}\}^{-1}\lambda^{ba}_{\vec\kappa}(1,1)(A^a_{\vec\kappa})^{s_1'}[\lambda^a_{\vec\kappa}(1)]^{-1}\Big), \quad s_1 \geqslant s_1' > 0. \tag{85}$$

For the particular case when both regions a and b constitute one-band sc crystals and the connection is as shown in Fig. 4(a), all quantities in (85) are scalars and $\lambda^a_{\vec\kappa}(1) = t_a$, $\lambda^b_{\vec\kappa}(1) = t_b$, and $\lambda^{ab}_{\vec\kappa}(1,1) = \lambda^{ba}_{\vec\kappa}(1,1) = t$, so that

$$\chi^{aa}_{\vec\kappa}(s_1, s_1'; z) = (zt_a)^{-1}\left[\sum_{r=0}^{s_1'-1} (A^a_{\vec\kappa})^{2r+s_1-s_1'+1} + \frac{t^2}{t_a t_b}(A^a_{\vec\kappa})^{s_1+s_1'}A^b_{\vec\kappa}\left(1 - \frac{t^2}{t_a t_b}A^a_{\vec\kappa}A^b_{\vec\kappa}\right)^{-1}\right], \quad s_1 \geqslant s_1' > 0. \tag{86}$$

For the sc regions we are considering, we have

$$\begin{aligned} u^a_{\vec\kappa}(s_1; z) &= \frac{1}{\pi}\int_0^\pi dk_1 \frac{\cos k_1 s_1}{1 - 2zt_a(\cos k_1 + \cos k_2 + \cos k_3)} \\ &= [1 - 2zt_a(\cos k_2 + \cos k_3)]^{-1}(1 - W^2)^{-1/2}W^{-s_1}[1 - (1 - W^2)^{1/2}]^{s_1}, \quad s_1 > 0, \end{aligned} \tag{87}$$

where

$$W = 2zt_a[1 - 2zt_a(\cos k_2 + \cos k_3)]^{-1},$$

and therefore

$$A^a_{\vec\kappa} = W^{-1}[1 - (1 - W^2)^{1/2}]. \tag{88}$$

The LDOS for the interface system we are considering is given by

$$D^\mu(s_1; E) = -\frac{1}{\pi}\mathrm{Im}\,E^{-1}J^{\mu\mu}(s_1, s_1, 0; E^{-1}), \quad \mu = a, b \tag{89}$$

where E has a small and positive imaginary part. From the structure of Eq. (86), we observe that this system can exhibit localized states, and that the wave vectors κ associated with these states are determined by the dispersion relation

$$1 - \tau A^a_{\vec\kappa}A^b_{\vec\kappa} = 0, \tag{90}$$

where $\tau = t^2/t_a t_b$. Moreover, since the boundary condition $u_{\vec\kappa}(s_1; z) \to 0$ as $s_1 \to \infty$ implies that $|A_{\vec\kappa}| < 1$, a necessary condition for the occurrence of localized states is that $\tau > 1$, i.e., the interface interaction must be greater than the geometric mean of the bulk interactions.

The contribution to the LDOS from the localized states is, from Eqs. (89) and (86), given by

$$\begin{aligned} D^\mu_{\mathrm{loc}}(s_1; E) &= -\frac{1}{\pi^3 t_\mu}\mathrm{Im}\int_0^\pi\!\!\int_0^\pi d\kappa \lim_{\eta\to 0^+}(A^\mu_{\vec\kappa})^{2s_1-1}[1 - \tau A^a_{\vec\kappa}A^b_{\vec\kappa} - i\,\mathrm{sgn}(A^\mu_{\vec\kappa})\eta]^{-1} \\ &= \frac{1}{\pi^2|t_\mu|}\int_0^\pi\!\!\int_0^\pi d\vec\kappa\,|A^\mu_{\vec\kappa}|^{2s_1-1}\delta(1 - \tau A^a_{\vec\kappa}A^b_{\vec\kappa}), \quad s_1 \geqslant 1. \end{aligned} \tag{91}$$

Using the δ-function property

$$\delta(f(\xi)) = \sum_i \left|\frac{df}{d\xi}\right|_{\xi=\xi_i} \delta(\xi - \xi_i),$$

where ξ_i are the zeros of $f(\xi)$, into Eq. (91), yields after some manipulation the expression

$$D^{\mu}_{\mathrm{loc}}(s_1;E)=\frac{1}{\pi^2|t_\mu|}\sum_i |A^{\mu}_{\vec{\kappa}}|^{2s_1-1}\left|\frac{\partial(1-\tau A^{a}_{\vec{\kappa}}A^{b}_{\vec{\kappa}})}{\partial\xi}\right|^{-1}_{\xi=\xi_i} K(1-(\xi_i/2)^2),\quad s_1\geq 1 \tag{92}$$

where $\xi=\cos k_2+\cos k_3$ and K is the complete elliptic function of the first kind.

We calculated the LDOS for the first two layers from each side of the interface. The LDOS was obtained through the numerical integration of Eq. (86) over the interface Brillouin zone. We chose two sets of values for the Hamiltonian parameters. In Fig. 10 we show results when $\epsilon_a=-\epsilon_b=1.5$; $t_a=-1.25$, and $t_b=-0.75$ in units of $|t|$. This set of values represents a metal joint

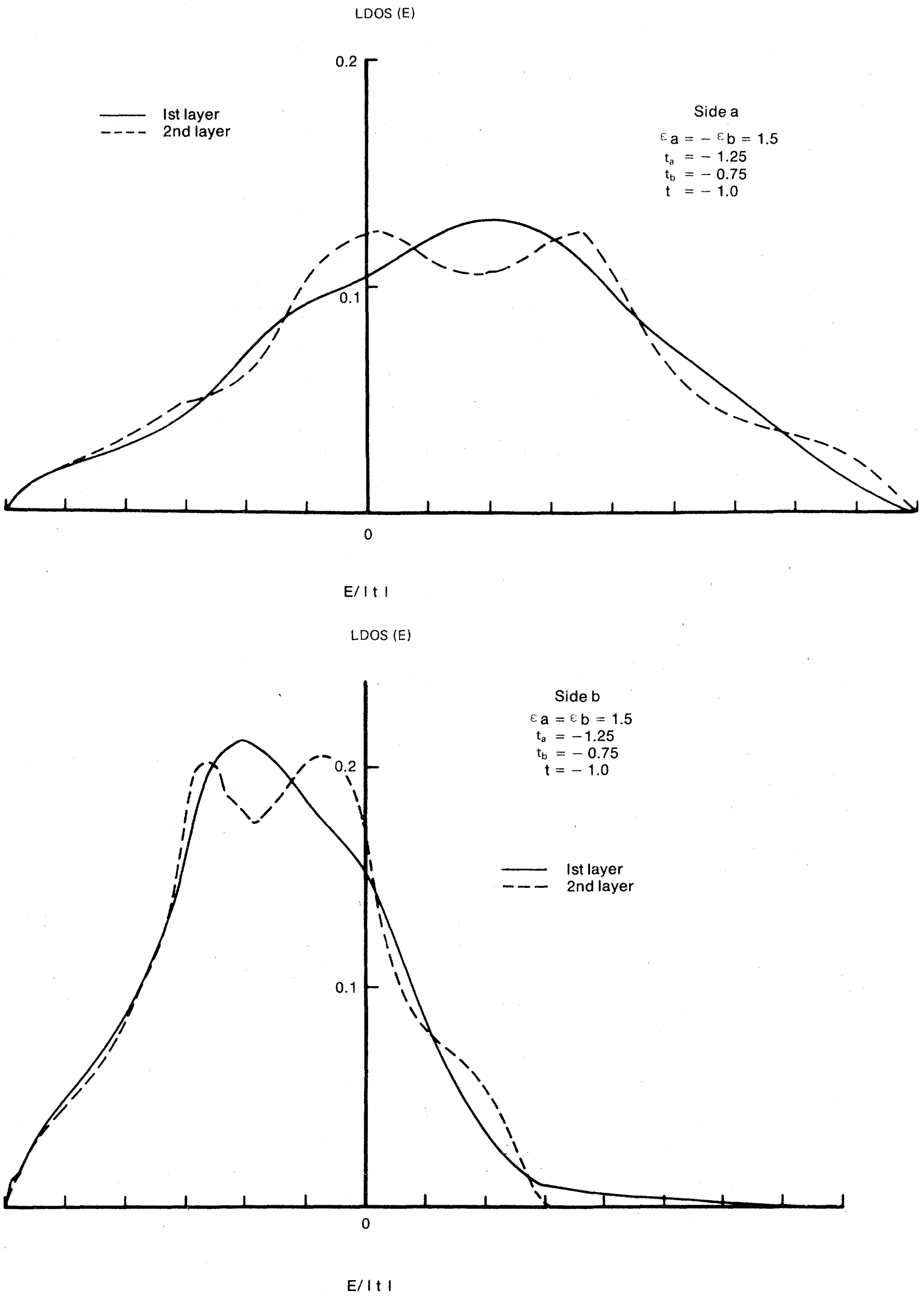

FIG. 10. LDOS for the first two layers from each side of the interface between two sc regions.

where the bandwidths for each region are similar, the main difference being the location of the band centers. The shapes of the curves shown in Fig. 10 closely resemble those for the LDOS of one-band sc (100) surfaces[1]; nevertheless, they differ from the latter by not being symmetrical with respect to the band centers. This distortion reflects the mixing of states from each region induced by the interface interaction, the effect being more pronounced for the first layer. Even though $\tau > 1$, the interface does not exhibit localized states. Our second choice of parameters was $\epsilon_a = -\epsilon_b = 0.1$, $t_a = -0.33$, and $t_b = -1.33$ in units of $|t|$. In this case the band widths are dissimilar, but the band centers almost coincide. In Fig. 11 we show the LDOS for bulk states. Now the LDOS does not resemble the semi-infinite, clean surface properties of each region. With this set of parameters we found localized states and their density of states, calculated from Eq. (92), is shown in Fig. 12.

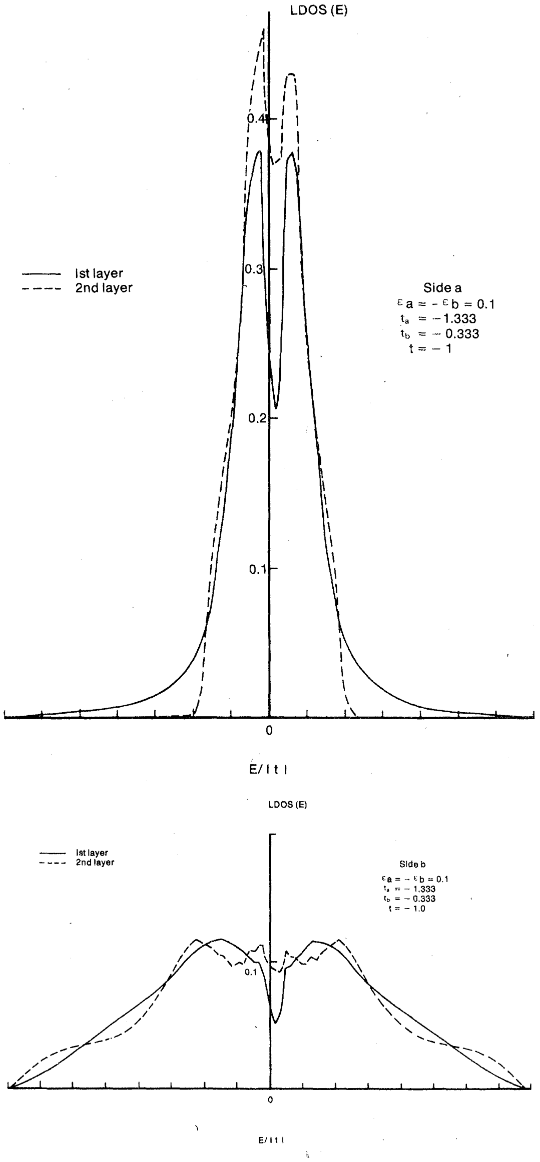

FIG. 11. Same as Fig. 10.

VI. SUMMARY

We have presented here a method for the exact calculation of the electronic Green's function associated with planar (unrelaxed) defects on crystals described by tight-binding Hamiltonians. We emphasized its use in the study of one-surface systems, thin films, and solid interfaces. The method is formulated in the language of random-walk theory, since the electronic Green's function can also be seen as a generating function for the probabilities associated with a stochastic process. By establishing its nature, that of a random walk on a lattice framework containing a set of traps, we have been able to derive expressions of considerable generality for the local Green's function in terms of that for the infinite system. This generality allowed us to consider mixed crystals with various interacting orbitals per atom and for interactions of arbitrary range.

For the case of one-surface crystals, we have shown that, under certain restrictions pertaining to the symmetry properties of the cleavage plane and the range of the interactions, the surface Green's function can be simply expressed as a difference of two bulk Green's functions. However, when these conditions are not satisfied it becomes necessary to use wave-vector-dependent bulk properties and the surface Green's function is obtained only after an integration over the SBZ. For the model of rocksalt we chose to exemplify surface calculations, we obtained the LDOS for the (100), (110), and (111) cleavage planes, and observed that the extent of band narrowing near the surface increases as the necessary number of bonds broken per atom to form the surface increases. As expected, for clean and unrelaxed surfaces with nearest-neighbor interactions,[1,2] the system does not show localized states.

In the case of thin films we obtained the local Green's function both as a series of bulk Green's functions and as a compact expression involving an integration over the SBZ. The latter proved to be useful for actual calculations, and in fact, for the bcc transition-metal film we examined, the LDOS was obtained in closed analytical form. This permitted a precise analysis of the singularities exhibited by the density of states. The relevant

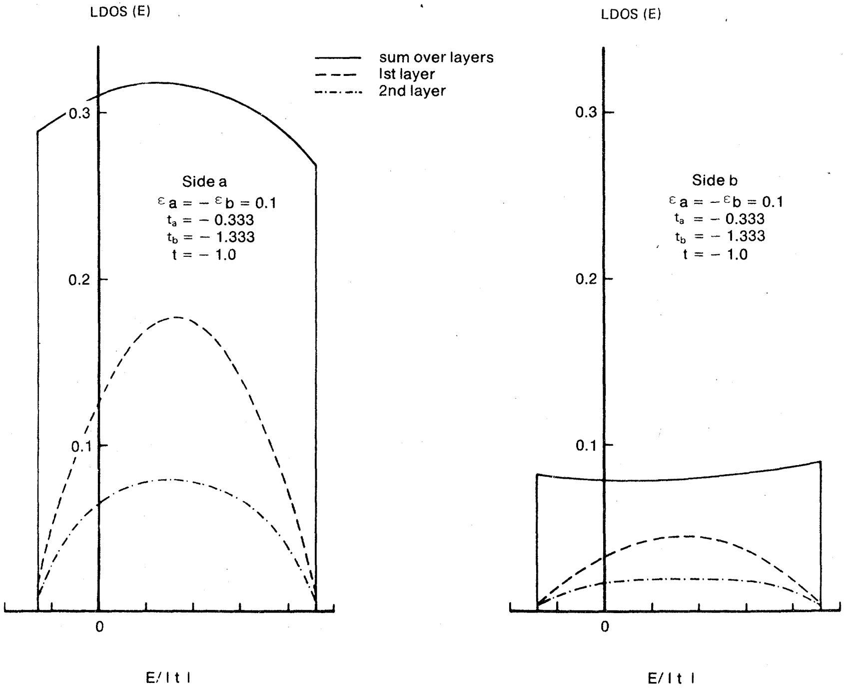

FIG. 12. Density of localized states for the first two layers from the interface, and for the sum over all layers of each side.

feature here was the alternating difference in the density of the *s* and *d* peaks, one increasing at the expense of the other, as one goes from one film layer to the next.

Our formalism for the LDOS does not require explicitly of the eigenstates of the system; nevertheless, for both semi-infinite and thin-film systems, the wave-vector dependence of these states was determined. Also, it is interesting to note that for the two-band models we studied, the final expressions for the local Green's function can be written in terms of the bulk Green's function for the corresponding one-band systems. This reduction can be accomplished in general for multiband crystals.

Exact tight-binding densities of states can be calculated for a large class of interface problems by means of our random-walk approach. Thus, for example, if we are interested in studying a system with two interfaces separating three different crystalline regions, it would be required to calculate separately the Green's functions for two semi-infinite regions and that for a film region. Subsequently, these functions can be progressively coupled, first, one of the semi-infinite regions with the film region to create one of the interfaces in a manner similar to that shown in Sec. V. The resulting Green's function would then be coupled with that of the remaining region to form the second interface. The method is equivalent to a repeated use of the Dyson equation.

Also, it is clear that the electronic properties of mono- or multilayer adsorption can be modeled in this manner. Here we illustrated the procedure for a simple model of a system with one solid interface, and found that the appearance of localized states is controlled by the geometry of the interface [see Eqs. (92) and (90)] and by the relative strength of the interactions at the interface when compared with those for the bulk regions.

These localized states were determined by inspection of the singularities appearing in the expression for the interface Green's function. The singularities are of two types. First there are those which originate from the bulk Green's function and therefore represent bulk states. But we also found others arising solely from the fact that the system contains an interface [see Eq. (90)]. The surface and film models we chose to study here only show singularities of the first type, but the consideration of relaxation effects would give rise to singularities of the second type. This procedure is equivalent to the so-called phase-shift method originally developed by De Witt[19] and subsequently applied by several authors to various modeled solid surfaces.[2,20] Also, the theory of Garcia-Moliner and Rubio[21] has been derived along similar lines. The main difference between these formalisms and ours is that they determine the localized state energies from a determinental equation involving only the bulk Green's function and the perturbation potential, whereas we actually calculate the local Green's function under consideration.

Finally, we have not considered here the effect that the relaxation of the surfaces (or interfaces) has on the LDOS of the system. However, these effects can be calculated by the method we have just described to study unrelaxed interfaces. Thus, for example, first-layer relaxation of a surface can be incorporated through the coupling of a monolayer film with an unrelaxed surface of the same material. The electronic energy at the first layer and the interaction through the "interface" could then be determined self-consistently for tight-binding Hamiltonians of the Hartree-Fock type.

The emphasis in this paper has been on development of techniques and methodology rather than on specific applications to real materials. In view of the fact that schemes more realistic than the tight-binding approximation can be employed with success to yield an improved LDOS (although few useful analytic results would be expected), such an effort might appear unjustifiable. However, the tight-binding approach shows considerable flexibility in incorporating surface relaxation and reconstruction effects,[1,2,10] thus allowing for a detailed analysis of how surface states arise.[1,2,20] Furthermore, this flexibility facilitates the study of such surface properties as, for example, local vibration frequencies,[22] where other methods lead to less tractable calculations. The work presented here may serve as a basis for these kinds of studies.

ACKNOWLEDGMENT

One of us (C. V.) would like to acknowledge partial support by Consejo Nacional de Ciencia y Technología, México 20, D. F., México.

---

[1] D. Kalkstein and P. Soven, Surf. Sci. 26, 85 (1971).

[2] W. Ho, S. L. Cunningham, W. H. Weinberg, and L. Dobrzynski, Phys. Rev. B 12, 3027 (1975).

[3] F. Cyrot-Lackmann, J. Phys. Chem. Solids 29, 1235 (1968); F. Cyrot-Lackmann, Adv. Phys. 16, 393 (1967).

[4] R. Haydock, V. Heine, and M. J. Kelly, J. Phys. C 5, 2845 (1972); R. Haydock and M. J. Kelly, Surf. Sci. 38, 139 (1973).

[5] F. Cyrot-Lackmann, J. Phys. (Paris) Suppl. C1, 67 (1970).

[6] F. Cyrot-Lackmann, M. C. Desjonqueres, and J. P. Gaspard, J. Phys. C 7, 925 (1974).

[7] Y. Muda and T. Hanawa, Surf. Sci. 66, 145 (1977).

[8] F. Ducastelle and F. Cyrot-Lackmann, J. Phys. Chem. Solids 31, 1295 (1970).

[9] M. C. Desjonqueres and F. Cyrot-Lackmann, Solid State Commun. 18, 1127 (1976).

[10] L. Dobrzynski and D. L. Mills, Phys. Rev. B 7, 2367 (1973).

[11] L. M. Falicov and F. Yndurain, J. Phys. C 8, 147 (1975); 8, 1563 (1975); F. Yndurain and L. M. Falicov, *ibid.* 8, 1571 (1975).

[12] B. Laks and J. B. Salzberg, Solid State Commun. 22, 417 (1977).

[13] T. L. Einstein, Phys. Rev. B 12, 1262 (1975); K. Masuda, Z. Naturforsch. A 31, 1344 (1976).

[14] K. Masuda, Z. Naturforsch. A 33, 66 (1978).

[15] E. W. Montroll and G. H. Weiss, J. Math. Phys. (N.Y.) 6, 167 (1965); E. W. Montroll, *ibid.* 10, 753 (1969); E. W. Montroll and H. Scher, J. Stat. Phys. 9, 101 (1973); A. Robledo and L. Woodhouse, *ibid.* 19, 129 (1978).

[16] C. Varea and A. Robledo, Phys. Rev. B 19, 1310 (1979).

[17] Although we do not refer explicitly to the assumed type of wave-function basis employed, the problem of atomic-like wave function overlap (like s-d overlap in transition metals) needs to be considered in some cases. One could instead assume a Wannier basis, thus by-passing the problem of nonorthogonality. On the other hand, nonorthogonality can be taken into account by introducing the following modifications in the random-walk algorithm. If θ denotes the relevant overlap matrix, the walker probabilities p and p_0 become $p = \theta H$ and $P_0 = \theta$, respectively.

[18] T. Morita and T. Horiguchi, J. Math. Phys. 12, 981 (1971).

[19] B. S. DeWitt, Phys. Rev. 103, 1565 (1956).

[20] G. Allan, Ann. Phys. (Paris) 5, 169 (1970); G. Allan and P. Lenglart, Surf. Sci. 15, 107 (1969); 30, 641 (1972).

[21] F. García Moliner and J. Rubio, J. Phys. C 2, 1789 (1969).

[22] C. M. Sayers (unpublished).